AD NUMBER
AD334089
CLASSIFICATION CHANGES
TO: unclassified
FROM: confidential
LIMITATION CHANGES
TO: Approved for public release, distribution unlimited
FROM: Controlling Organization: British Embassy, 3100 Massachusetts Avenue, NW, Washington, DC 20008.
AUTHORITY
DSTL, ADM 302/88, 18 Nov 2008; DSTL, ADM 302/88, 18 Nov 2008

A. U. W. E. Tech Note 88/62

334089

CATALOGED BY ASTIA AS AD No. ___

CONFIDENTIAL

U.D C. No
623.863

A. U. W. E. Tech Note 88/62

ACSIL/ADM/62/ 238

COPY No 58

SHIPS' PRESSURE FIELDS.

BY
S. COAD.

"This document is the property of H.M. Government and is issued for the information of officers. The officer in possession of this document is responsible for its safe custody and that its contents are not disclosed to any unauthorised person. It must be kept under lock and key when not in use and any loss or destruction must be reported to the originating Establishment through normal channels".

ADMIRALTY UNDERWATER WEAPONS ESTABLISHMENT

PORTLAND

"Excluded From Automatic Regrading; DOD Dir 5200.10 Does Not Apply"

CONFIDENTIAL

CONDITIONS OF RELEASE

This information is disclosed only for official use by the recipient Government and such of its contractors, under seal of secrecy, as may be engaged on a defence project. Disclosure to any other Government or release to the Press or disclosure in any other way would constitute a breach of these conditions. The information should be safeguarded under rules designed to give the same standard of security as maintained by Her Majesty's Government in the United Kingdom. The recipient is warned that information contained in this document may be subject to privately-owned rights.

The views expressed herein do not necessarily represent the considered opinion of the issuing Establishment and must not be taken to define Admiralty or Departmental policy.

U.D.C. No. 623.863

A.U.W.E. Technical Note 88/62
July 1962

SHIPS' PRESSURE FIELDS

by

S. Coad

-oOo-

DISTRIBUTION

	Copy No.
D.G.W.(U), Bath	1 to 2
C.R.N.S.S.	3
D.P.R.	4
A.E.W.	5
A.R.L.	6
Captain, H.M.S. VERNON	7
Secretary, Naval Board Military Agency for Standardisation (for distribution to N.A.T.O. Countries)	8 to 47
A.C.S.I.L.	48 to 77

CONTENTS

LIST OF TABLES

U.D.C. No. 623.863

A.U.W.E. Technical Note 88/62
July 1962

SHIPS' PRESSURE FIELDS

by

S. Coad

-oOo-

DISTRIBUTION

	Copy No.
D.G.W.(U), Bath	1 to 2
C.R.N.S.S.	3
D.P.R.	4
A.E.W.	5
A.R.L.	6
Captain, H.M.S. VERNON	7
Secretary, Naval Board Military Agency for Standardisation (for distribution to N.A.T.O. Countries)	8 to 47
A.C.S.I.L.	48 to 77

CONTENTS

LIST OF TABLES

LIST OF FIGURES

LIST OF SYMBOLS

P	The peak pressure-reduction occurring in a ship's signature.
P_{xy}	The pressure change on the sea-bed at a point x abaft the bow and y abeam of the track.
P_y	The peak pressure reduction occurring at a distance y abeam.
θ	The duration of reduced pressure.
θ_L	The time taken for a ship's length between perpendiculars to pass.
h	Depth of water.
L	Length of ship between perpendiculars.
V	Speed of ship.
ρ	Density of water.
C_p	Prismatic coefficient of hull.
∇	Displacement volume of hull.

LIST OF SYMBOLS (Contd.)

Δ		Displacement mass of hull. ($\Delta = \rho\nabla$).
g		Acceleration due to gravity.
Υ	=	$V/\sqrt{gh}$, the ratio of ship's speed to the critical wavemaking speed.
F	=	Fullness Ratio
F'	=	Modified Fullness Ratio

$\left.\begin{matrix} F \\ F' \end{matrix}\right\}$ defined in paragraphs 45 and 47.

SHIPS' PRESSURE FIELDS

PRÉCIS

1. Detailed predictions of the pressure field of a ship may be made by the methods of Reference 1. This, however, involves lengthy numerical computation for each ship and each set of conditions and it is desirable to have, if possible, simple formulae which relate, if only approximately, the most important features of the pressure field to parameters representing the form of the ship's hull.

2. Dimensional analysis suggested the form which such relations might take and basic data derived from observation and from the detailed theory were duly examined.

3. The peak suction P, the suction duration θ and the quantity $P\theta^2$ may be expressed in terms of two hull-shape parameters. Other important features, concerning pressure signature shape and relevant to the actuation of 'simple' and 'integrating' mines, may also be estimated.

CONCLUSIONS

4. Important features of the pressure change on the sea-bed due to a passing ship may be estimated either from simple formulae or from universal curves. The ship is described sufficiently by two hull-shape parameters of a type familiar to naval architects - the prismatic coefficient and the ratio: displaced volume to length cubed.

INTRODUCTION

5. The pressure change on the sea-bed due to a passing ship may be predicted from the theory of References 1 and 2. This, however, requires lengthy numerical computation for each hull and each set of conditions, but in pressure mine countermeasures work it is desirable to have expressions which, even if not highly accurate, afford a means of rapidly assessing significant features of any ship's signature. Now, whereas the detailed computations start from detailed information as to the curve of underwater section areas of the hull, it seems that ships in general are sufficiently alike to be characterised individually by a small number of shape parameters.

6. Features of the pressure field which are of particular importance are the peak suction P, the duration of suction θ, and the combined magnitude $P\theta^2$. Knowledge of these quantities, which apart from ship's shape are affected also by depth, distance abeam and speed, is sufficient for the estimation of safe-speeds against simple pressure mines. The report describes regularities noticed in the dependence of these quantities on the conditions and presents simple approximate formulae.

7. The substance of the report was communicated in an informal presentation to the N.A.T.O. Mine Countermeasures Working Party Panel of Technical and Scientific Experts at their meeting in Paris in October 1961.

CHOICE OF DIMENSIONLESS PARAMETERS

8. A dimensional analysis suggests that the pressure at any point (x,y) in a ship's pressure field should be capable of expressions in the form:-

$$\frac{P_{xy}}{\frac{1}{2}\rho V^2} = f\left(\frac{x}{L}, \frac{h}{L}, \frac{y}{L}, \frac{V}{\sqrt{gL}} + \text{hull shape parameters}\right),$$

where f symbolises some unknown functional dependence. It is clear that in this form of expression the absolute size of ship is unimportant, the dimensionless pressure being decided by geometrical relationships expressing the ratios of characteristic lengths.

9. In principle, to cater for all possible hull shapes it would be necessary to include an infinite number of shape parameters, however it appeared that hulls of conventional form would be permitted little scope for variation if both C_p and ∇/L^3 were fixed. C_p broadly fixes the rates of growth and decay of the underwater section area along the ship's length, but a fixed C_p alone would not locate a ship in the range from short and bluff to long and slender. This degree of freedom is eliminated by specifying ∇/L^3. Thus it was hoped that regularities based on the following expression might be discovered:-

$$\frac{P_{xy}}{\frac{1}{2}\rho V^2} = f\left(\frac{x}{L}, \frac{y}{L}, \frac{h}{L}, \frac{V}{\sqrt{gL}}, C_p, \nabla/L^3\right)$$

10. Since the peak suction rather than the detailed variation of pressure throughout a signature is of direct interest the term x/L may be omitted.

Finally, instead of $\frac{V}{\sqrt{gL}}$ it is convenient to substitute the quantity

$$\gamma = \frac{V}{\sqrt{gh}}$$, where $\sqrt{gh}$ is the critical wavemaking speed.

11. These considerations suggest that a search for simple regularities should be guided by the expression:-

$$\frac{P_y}{\frac{1}{2}\rho V^2} = f\left(\frac{h}{L}, \frac{y}{L}, \gamma, \frac{\nabla}{L^3}, C_P\right).$$

A similar expression would be expected to govern other dimensionless parameters, such as θ/θ_L, associated with the pressure signature.

THE BASIC DATA

12. It was intended initially that the investigation should be purely experimental and as a beginning four model merchant ships were made and pressure-ranged in the A.U.W.E. Miniature Ship Tank. Apart from some difficulties in interpretation of the pressure signatures of these small models, which were later resolved (Reference 4), it was clear that experimental scatter would tend to obscure any relationships and necessitate a long programme of measurements. Since the detailed theory and observation had been shown to be broadly consistent (Reference 5) and a digital computer was available to speed computation, it was decided to adopt the complementary approach of computing signatures for a methodical series of hull shapes. These would not be subject to experimental scatter and, even if the predictions only approximate the truth, their consistency should aid the discovery of semi-empirical rules.

13. Accordingly the pressure fields of three hull shapes belonging to the D.T.M.B. series 60 (Reference 6) and having different values of C_P were computed. Table 1 gives details of the hull shapes and Figures 1 to 12 show keel signatures for various values of h/L and for two values of γ(0.1 and 0.4). The theoretical expression (Reference 1) which leads to the keel signatures may be written:-

$$\frac{P_x}{\frac{1}{2}\rho V^2} = -\frac{1}{1-\gamma^2} \cdot \left(\frac{h}{L}\right)^{-2} \cdot \frac{\nabla}{L^3} \cdot \frac{1}{C_P} \cdot \frac{1}{\pi}\int_0^{L/h} \frac{A(t)}{A_M} G\left\{\frac{t - \frac{L}{h}\frac{x}{L}}{\sqrt{1-\gamma^2}}\right\} dt,$$

where A_M = maximum underwater section area of hull

A_t = section area at longitudinal station distant tL from forward perpendicular

function G is proportional to the pressure contribution at x on the sea-bed from a doublet of strength A(t)dt at position tL.

14. It is clear that, for a given C_P, variation of hull shape as regards ∇/L^3 simply generates a family of signatures in which the pressures are proportional to ∇/L^3. On the other hand the situation as regards C_P, for a

given ∇/L^3, is less simple in principle because variation of C_P affects the factor $A(t)/A_M$ in the integrand. It was sufficient in the computation therefore to examine the effects of varying only C_P.

15. A further source of data was a miscellaneous collection of computations and measurements in respect of various ships and derived from various sources. Some of this information was of doubtful value owing to omissions and it was realised that scatter could be caused, for instance, by overlooked differences in the definition or evaluation of the parameters - differences, for example, between waterline length and length between perpendiculars, between nominal and actual displacement.

THE PEAK SUCTION

16. In this section the dependence of peak suction upon the parameters, taken as far as possible separately, is examined. To some extent this does not reflect the actual procedure which first suggested the correlations, in that a rule for one parameter having been found the data may be reduced accordingly and made available for exhibiting other regularities.

Dependence on Depth

17. Table 2 shows measured data for the four model merchant ships at six depths in the range $0.094 \leqslant h/L \leqslant 0.625$. A tentative reduction of the data in regard to γ and ∇/L^3 has been made and the results are averaged to show the simple power law dependence upon depth illustrated in Figure 13. The index is very nearly minus 1.5.

18. The result of a similar reduction of the data for the Series 60 ships is shown in Figure 14. Here the data have been tentatively reduced with regard also to C_P. A $(\text{depth})^{-1.5}$ law would fit very well over a substantial range but a moderate disagreement is evident at the larger depths. This is not revealed in the experimental results but these do not extend to great enough depths to establish a distinct discrepancy.

Dependence on γ

19. It was known that at very low speed the pressures in a signature are accurately proportional to V^2 but that at higher speeds the actual values exceed the extrapolated ones by an increasing fractional discrepancy. The theory of Reference 1 is limited to values of $\gamma < 0.4$ but even so the manner of the dependence upon γ cannot be extracted in simple form from the expression of paragraph 13. The theoretical expression suggests that the residual dependence of

$$p\,\frac{(1-\gamma^2)}{\frac{1}{2}\rho V^2} \text{ upon } \gamma$$

should be investigated.

20. Figure 15 shows the results of an experiment on one of the model merchant ships in which γ was varied between 0.2 and 0.43. Strictly the experiment indicates, as was to be expected, that a varying "n" would be necessary according to the range of γ to be covered by a law of the form:

$P = k(1-\gamma^2)^n$. Factors bearing on the choice of a suitable value for n were:-

(a) There is some dependence on γ (i.e. $n \neq o$).

(b) For small γ the dependence is not sensitive to the precise value of n.

(c) At small γ, $n \doteq -1$; at larger values $|n|$ increases to 2 or more.

$n = -1$ was chosen because:-

(d) Only small errors ($\sim 3\%$) would be involved for values of γ up to 0.4, provided the numerical coefficient were suitably chosen.

(e) $n = -1$ is simple.

(f) The computed values for Series 60 ships for $\gamma = 0.1$ and $\gamma = 0.4$ show good agreement if reduced according to $(1-\gamma^2)^{-1}$. This is shown in Table 3 which indicates that the variation with γ does not depend upon the shape of ship but does depend slightly on depth. However, the mean value of the ratio of pressures between the different values of γ is quite consistent with the $(1-\gamma^2)^{-1}$ law. But the curvature shown in Figure 15 suggests that this accurate agreement may be a fortuitous consequence of the particular values of γ chosen.

21. A more thorough examination of the dependence of P upon γ might perhaps be profitable but it is clear that the fitting of a $(1-\gamma^2)^{-1}$ law avoids the significant error which would result from completely ignoring the γ dependence, and for practical purposes this "first order compensation" is probably adequate. Moreover the recognition of this dependence serves as a reminder that the simple speed-squared law fails badly at high speed even though prediction will not then be accurate.

Dependence on ∇/L^3

22. The theory indicates that the pressure at a given abscissa should vary directly with ∇/L^3 and it follows that the peak suction will vary in the same way.

23. Experimental evidence confirms this. For example it had been noticed that the relative scatter in the entries of Table 2 was considerably reduced by the inclusion of the factor L^3/∇, and in order to examine the matter further the displacement of one of the model merchant ships was deliberately varied over a wide range by changing the ballast. The variation of peak suction with displacement is shown in Figure 16. A straight regression line fitted to the experimental points has a slightly smaller slope than a line joining their mean to the origin, but this is attributable to the marginal and unavoidable changes of C_P and L that were associated with the variation of ∇. This was confirmed by examining the ratio between the pressures associated with the normal displacement (567 grammes) and with a large displacement (810 grammes). Values of C_P and L were reassessed for the larger displacement from the ship's sheer drawings. The formula of paragraph 28 accounts within $\sim 2\%$ for the observed value of the ratio.

Dependence on C_P

24. The data originally tested, i.e. model merchant-ship data and miscellaneous computations, did not, owing to a moderate scatter, give a clear indication of the dependence on C_P. Of two tested relationships, of the form PC_P = const. and PC_P^2 = const., the evidence favoured the latter but this, as it turned out, was misleading. Figure 17 shows the way in which the alternative parameters based on the limited data depend on C_P. Some of the scatter here is due to imperfection of the compensation for depth by means of the factor $(h/L)^{3/2}$. However, it is clear that for the points which have C_P to the first power in the ordinate expression there is a residual dependence on C_P which is apparently removed by using the factor C_P^2 instead.

25. Only when other data were tested did it become clear that a simple C_P law would be better. It was then appreciated that the original data for the higher prismatic coefficients had been observed and those for the lower, computed. This could account for the distinct regression shown by the "C_P points" because there is some evidence (Reference 5) that the theory slightly overestimates. The discrepancy illustrates the risk which is involved in basing statistical conclusions on non-homogeneous data.

26. With regard to the Series 60 ships Table 4 shows that, except perhaps at the greatest depths, the value of $C_P.P$ is substantially uniform over the range of C_P. A graph of the values plotted against depth is shown in Figure 18, which also displays the results of computations for various actual hull shapes with C_P ranging from 0.547 to 0.8.

The Joint Dependence

27. It appears from the foregoing discussion that an expression of the form:-

$$\frac{P(1-\gamma^2)}{\frac{1}{2}\rho V^2}\,\frac{L^3}{\nabla}\,.\,C_P = f\left(\frac{h}{L}\right),$$

should hold approximately for all ships. That it does so is strongly suggested by Figure 19 which displays miscellaneous results, both observed and computed, for many ships. Some, at least, of the quite small scatter arises from lack of homogeneity in the data. The drawn curve was sketched through the mean computed points for the Series 60 ships.

28. In the range $0.1 < h/L < 0.5$, which covers many practical cases and most of the data, the curve is well approximated by the formula:-

$$\frac{P(1-\gamma^2)}{\frac{1}{2}\rho V^2}\,.\,\frac{L^3}{\nabla}\,.\,C_P = 0.76\left(\frac{h}{L}\right)^{+3/2},$$

which is represented by the straight line in the logarithmic plot of Figure 14. It will be noticed that the actual values depart from the line by about 7% at the extremes of the quoted range - the formula overestimating. At the middle of the range there is a 2% underestimation.

The Effect of Distance Abeam

29. For a given ship, speed and depth the peak suction falls off at points away from the keel-line. The variation is shown for two values of C_P in Figure 20. The simple source-sink representation yields (Appendix B) an asymptotic expression valid for large distances abeam and vanishingly small values of γ. Allowing for the anticipated variation with γ discussed above this suggests the following expression:-

$$\frac{P(1-\gamma^2)}{\frac{1}{2}\rho V^2} = \frac{1}{\pi} \cdot \frac{\nabla}{L^3} \cdot \frac{L}{h}\left[\frac{1}{y^2/L^2 + C_P{}^2/4}\right]$$

provided $y^2/L^2 + C_P{}^2/4 - 2h^2/L^2 > 0$.

That it in fact holds is shown for two Series 60 ships in Table 7. For most practical purposes estimation from the diagram of Figure 20 would suffice, since the curves are independent of ∇/L^3 and there is not a marked dependence on C_P.

THE QUANTITY $P\theta^2$

30. $P\theta^2$ is important in pressure mine countermeasures because it is substantially independent of speed of ship and is therefore capable of representing a ship while safe speeds are being determined. In order to establish the dependence on the other parameters it was decided to examine the behaviour of the dimensionless quantity:-

$$\frac{P}{\frac{1}{2}\rho V^2}\left(\frac{\theta}{\theta_L}\right)^2$$

Variation of $P\theta^2$ on the Keel Line

31. Table 5 shows factors of the above expression for the Series 60 ships and for N.A.V. Spa, for a range of h/L and for two values of γ. It was noticed that the inclusion of the further factor $(1-\gamma^2)^{\frac{1}{2}}$ effectively removes the dependence on γ (Column 6).

32. On making a logarithmic plot of Column 6 against Column 2 it appeared that the data for each ship could be accurately represented by a law of the form:-

$$\frac{P}{\frac{1}{2}\rho V^2}\left(\frac{\theta}{\theta_L}\right)^2 (1-\gamma^2)^{\frac{1}{2}} \left(\frac{h}{L}\right)^{1.08} = \text{Constant.}$$

33. The data were then examined to see whether the variation from ship to ship could be expressed in terms of the hull shape parameters. It was noticed that this could be accomplished by reference to ∇/L^3 alone, the variation of C_P being of no account. (Figure 21).

34. At medium and large depths the expression:-

$$\frac{P}{\frac{1}{2}\rho V^2}\left(\frac{\theta}{\theta_L}\right)^2 = 1.51\left(\frac{h}{L}\right)^{-1.08} \frac{\nabla}{L^3}(1-\gamma^2)^{-\frac{1}{2}}$$

fits the data very well, but at depths for which the pressure signatures show two minima the greatest suction is somewhat greater than implied by the above expression, whereas the suction at the turning point (the relative-maximum of pressure) near the middle of the signature is somewhat less. When a signature has more than one minimum the peak-suction is no longer the obvious choice to represent the general suction magnitude. A one-parameter representation clearly has shortcomings and it is fortunate that the simple law predicts reasonable intermediate values. It is found that if, for such signatures, P is taken to mean:

$\frac{1}{2}$(Absolute Minimum Pressure + Relative Maximum Pressure)

then the above expression fits very well throughout at least the range: $0.1 < h/L < 0.8$. In Table 5 (Columns 7 and 8) this value is given in parentheses, where it differs from the peak value.

35. Column 8 of Table 5 shows actual values - the bracketed values are those defined as above for "double humped" signatures. The accuracy with which this simple law seems to hold is all the more remarkable when it is recalled that P and θ separately do not obey simple depth-laws over such a wide range.

36. It is possible without excessive error to represent the data by a simple inverse-depth law:-

$$\frac{P}{\frac{1}{2}\rho V^2}\left(\frac{\theta}{\theta_L}\right)^2 = 1.7\left(\frac{h}{L}\right)^{-1}\frac{\nabla}{L^3}\,(1-\gamma^2)^{-1} .$$

37. At low speeds (γ small) this expression in turn leads to the following practical formula for keel signatures:-

$$P\theta^2 \doteqdot 11.2\,\frac{\Delta}{h}\ \text{inch water. sec}^2$$

where Δ is the ship's displacement in tons and h the depth in feet. At $h/L = 0.1$ the magnitude predicted from the simplified expression would be about 13% low, and at $h/L = 0.8$ it would be about 13% high.

<u>The Effect of Distance Abeam</u>

38. The variation of dimensionless $P\theta^2$ with distance abeam is shown for various depths in Figures 22, 23 and 24. It appears that at large distances abeam the values level out, and it was noticed that the levels could be accurately represented by the expression:-

$$\left[\frac{P}{\frac{1}{2}\rho V^2}\cdot\left(\frac{\theta}{\theta_L}\right)^2\right]_{\text{REMOTE}} = 1.29\,\frac{\nabla}{L^3}\cdot\left(\frac{h}{L}\right)^{-1}\cdot(1-\gamma^2)^{-1} .$$

39. It is of interest to note that this semi-empirical expression is quite consistent with the magnitude predicted from a simple source/sink representation of a ship, if the separation of source and sink is taken to be $C_p L$. (See Appendix A). The simple theory then leads to a numerical coefficient of $4/\pi$ ($\doteqdot 1.273$).

40. Ignoring the gentle dependence on γ, and using the approximate expression for the keel line, we can write the following expression for the range of athwartships variation of $P\theta^2$:-

$$\underset{\text{Remote}}{1.29\frac{\nabla}{L^3}\left(\frac{h}{L}\right)^{-1}} < \frac{P}{\frac{1}{2}\rho V^2}\left(\frac{\theta}{\theta_L}\right)^2 < \underset{\text{Keel Line}}{1.7\frac{\nabla}{L^3}\left(\frac{h}{L}\right)^{-1}}$$

which in practical units leads to:-

$$8.5\frac{\Delta}{h} < P\theta^2 < 11.2\frac{\Delta}{h}\text{ inch water. sec}^2$$

where Δ is expressed in tons and h in ft.

THE DURATION OF SUCTION θ

Keel Line Case

41. The expressions for P and $P\theta^2$ given in paragraphs 28 and 34 lead to an expression for θ:-

$$\frac{\theta}{\theta_L} = 1.39\left(\frac{h}{L}\right)^{1/5} C_p^{\frac{1}{2}}\left(1-\gamma^2\right)^{\frac{1}{2}}$$

provided the limitation of paragraph 28 is observed (i.e. $0.1 < h/L < 0.5$); it being expected that the predicted value would be some $3\frac{1}{2}\%$ low at the extremes of the range and slightly high at the middle. Values given by this expression and by detailed calculation are compared for a few cases in Table 6.

The Effect of Distance Abeam

42. The variation of θ, relative to the keel line value, not θ_L, is shown for a range of relative beam-distances in Figure 25. It is clear that at moderate and large distances abeam there is a substantial dependence on C_P.

43. It is noted that the expression:-

$$\frac{P}{\frac{1}{2}\rho V^2}\left(\frac{\theta}{\theta_L}\right)^2 = 1.29\left(\frac{h}{L}\right)^{-1}\frac{\nabla}{L^3}\left(1-\gamma^2\right)^{-\frac{1}{2}}$$

fits very well at large distances abeam, and so does the expression:-

$$\frac{P}{\frac{1}{2}\rho V^2} = \frac{1}{\pi}\left(\frac{h}{L}\right)^{-1}\frac{\nabla}{L^3}\left(\frac{1}{y^2/L^2 + C_p{}^2/4}\right)\left(1-\gamma^2\right)^{-1} .$$

Whence:-

$$\frac{\theta}{\theta_L} \doteqdot 2\left(y^2/L^2 + C_p{}^2/4\right)^{\frac{1}{2}}\left(1-\gamma^2\right)^{\frac{1}{4}} ,$$

which shows the same dependence on γ as in the keel line case.

44. As might be expected, for sufficiently large distances abeam a simple source-sink representation of the ship predicts the value of θ accurately for the case when $\gamma \rightarrow 0$ (see Appendix A).

THE SHAPES OF PRESSURE SIGNATURES

45. It is clear upon examining an assortment of pressure signatures that the suction part of the signature takes various shapes, according to the conditions, from a quasi-rectangular form to a quasi-triangular form. For given peak suction and duration of suction the first shape would be more likely to actuate a Simple Pressure Mine than the second. Signatures may be ordered in this connection by associating with each a "Fullness Ratio" F defined as follows:-

$$F = \frac{\text{Time integral of suction}}{P\theta} .$$

A rectangular signature would give F = 1, and a triangular F = 0.5.

46. The variation of F with C_P and depth is shown in Figure 26 for keel signatures. Figures 27 and 28 show the effect of distance abeam. It appears that at large relative distances from the ship, F tends to the same, relatively low, value (~ 0.53) regardless of the shape of ship.

Shape in Relation to "Integrating Mines"

47. If an integrating feature were included in a pressure mine in order to eliminate dependence on the speed of the target it is likely that the mine would be arranged to sense the magnitude of

$$\int (\text{suction})^{\frac{1}{2}}\, dt.$$

So that signatures may be ordered also in this connection a modified fullness ratio F' is appropriate:-

$$F' = \frac{\text{Time integral of (suction)}^{\frac{1}{2}}}{P^{\frac{1}{2}}\,\theta} .$$

Figures 29 and 30 show that this quantity varies between 0.67 and 0.86.

48. Since $P\theta^2$ and hence $P^{\frac{1}{2}}\theta$ are readily determined (paragraph 34) a knowledge of F' leads immediately to an estimate of the integral. Taking the approximate expression, for the keel line, we have for the range of variation athwartships:-

$$\underset{\text{Abeam}}{F' \sqrt{8.5\,\frac{\Delta}{h}}} < \int P^{\frac{1}{2}}\, dt < \underset{\text{Keel}}{F' \sqrt{11.2\,\frac{\Delta}{h}}} . \quad (\text{inch water})^{\frac{1}{2}}.\ \text{sec}$$

if Δ is expressed in tons and h in feet. Or, inserting the appropriate values of F':-

$$2\sqrt{\frac{\Delta}{h}} < \int P^{\frac{1}{2}}\, dt < 3\sqrt{\frac{\Delta}{h}}\ (\text{inch water})^{\frac{1}{2}}.\text{sec}.$$

REFERENCES

Reference

1 The Pressure Fields of Moving Bodies
U.C.W.E. Informal Report 1540/52
" " " 1563/52

2 Foxwell, J.H. - The Calculation of Ships' Pressure Fields - A.U.W.E. Technical Note No.29/61. (SECRET).

3 The Pressure Fields of Moving Bodies - Interim Report - U.C.W.E. Informal Report No.1514/51. (SECRET).

4 Coad, S. - Model Scale Effect on Ships' Pressure Fields - A.U.W.E. Technical Note No.46/61. (CONFIDENTIAL).

5 Coad, S. - Ships' Pressure Fields. A Comparison Between Theory and Observation - A.U.W.E. Technical Note No.50/61. (CONFIDENTIAL).

6 Trans. Soc. Naval Architects and Marine Engineers. Vol.61 1953.

L.G.H.

APPENDIX A: SIMPLE THEORY

1. In this appendix the assumptions of Reference 3 are adopted, namely that the ship can be represented by a single source and single sink and that the water surface can be treated as plane and rigid.

2. Reference 3 shows that:-

$$P_{xy} = \frac{AV^2}{2\pi gh}\left\{\frac{x - L_e/2}{y^2 + (x-L_e/2)^2} - \frac{x + L_e/2}{y^2 + (x+L_e/2)^2}\right\} \text{ head of fluid units,}$$

provided:-

$$\left|\left[y^2 + (x-L_e/2)^2\right]^{\frac{1}{2}}\right| > \sim 1.4h$$

$$\text{and } \left|\left[y^2 + (x+L_e/2)^2\right]^{\frac{1}{2}}\right| > \sim 1.4h .$$

(The origin is midway between source and sink, and L_e is the separation of source and sink. 'A' is the midships cross sectional area of the ship). Hence $P_{xy} = 0$ when:-

$$\frac{x - L_e/2}{y^2 + (x-L_e/2)^2} = \frac{x + L_e/2}{y^2 + (x+L_e/2)^2}$$

i.e. when:-

$$x = \pm\sqrt{y^2 + L_e^2/4} \; .$$

Since $\theta = \frac{2x}{V}$, then:-

$$\theta^2 = \frac{4}{V^2}(y^2+L_e^2/4)$$

Again, $P = P_{oy} \doteqdot \frac{AV^2}{2\pi gh}\left(\frac{L_e}{y^2+L_e^2/4}\right)$ head of fluid units

whence $P\theta^2 = \frac{2AL_e}{\pi gh}$ head.time^2

or $\frac{2\rho AL_e}{\pi h}$ pressure.time^2.

This is independent of distance abeam, y, provided the above conditions are satisfied. Making this expression dimensionless, by reference to the dynamic pressure and the time taken for the ship's length <u>between perpendiculars</u> to pass, we have:-

$$\frac{P\theta^2}{\frac{1}{2}\rho V^2(L/V)^2} = \frac{4AL_e}{\pi hL^2} \; .$$

Put:-

$$L_e = kC_pL.$$

Then, since $C_pAL = \nabla$:-

$$\text{dimensionless } P\theta^2 = \frac{4k\ \nabla/L^3}{\pi\ h/L}.$$

Comparing this with the expression in paragraph 38 it is seen that there is good consistency if $k = 1$, i.e. if $L_e \equiv C_pL$; and if $\gamma \to 0$. There are independent reasons, incidentally, for identifying the effective source-sink separation with C_pL. (Reference 1). (The simple theory, in assuming a plane water surface, cannot of course indicate the dependence on γ, and it would be expected to make valid predictions, if at all, only when $\gamma \to 0$.)

APPENDIX B: FURTHER APPLICATION OF SIMPLE THEORY

1. The success of the simple source-sink theory in predicting the value of $P\theta^2$ on the beam (Appendix A) prompts the enquiry whether there would be similar success in predicting P if the identification: $L_e \equiv C_p L$ were again made.

2. We have, as in Appendix A:-

$$P_{oy} = \frac{AV^2}{2\pi gh}\left(\frac{L_e}{y^2+L_e^2/4}\right) \text{ head of fluid.}$$

$$= \frac{C_p L\, AV^2}{2\pi gh}\left(\frac{1}{y^2+C_p^2 L^2/4}\right)$$

$$= \frac{\nabla}{L^3}\cdot\frac{V^2}{2g\pi}\cdot\frac{L}{h}\left(\frac{L^2}{y^2+C_p^2L^2/4}\right),$$

since $C_p LA = \nabla$.

Rearranging and expressing in fundamental units:-

$$\frac{P_{oy}}{\frac{1}{2}\rho V^2} = \frac{1}{\pi}\;\frac{\nabla}{L^3}\cdot\frac{L}{h}\left(\frac{1}{y^2/L^2+C_p^2/4}\right).$$

3. It can be shown from the restrictions quoted at the beginning of Appendix A that this expression would be expected to hold within about 10% provided:-

$$y^2/L^2 - 2h^2/L^2 + C_p^2/4 > 0.$$

TABLE 1: D.T.M.B. SERIES 60 HULLS
DISTRIBUTION OF SUBMERGED SECTION AREA

x/L	Model 4210 W $C_p = 0.614$	Model 4212 W $C_p = 0.710$	Model 4214 W-B4 $C_p = 0.805$
	Fraction of Midships Section Area		
0(F.P.)	0	0	0
1/32	0.041	0.094	0.293
2/32	0.109	0.213	0.545
3/32	0.177	0.339	0.713
4/32	0.255	0.477	0.833
5/32	0.342	0.603	0.912
6/32	0.433	0.715	0.961
7/32	0.531	0.807	0.987
8/32	0.630	0.881	0.997
9/32	0.721	0.937	1.000
10/32	0.800	0.968	1.000
11/32	0.869	0.988	1.000
12/32	0.923	0.998	1.000
13/32	0.961	1.000	1.000
14/32	0.984	1.000	1.000
15/32	0.998	1.000	1.000
16/32	1.000	1.000	1.000
17/32	0.998	1.000	1.000
18/32	0.991	1.000	1.000
19/32	0.980	0.995	1.000
20/32	0.960	0.988	1.000
21/32	0.929	0.971	0.997
22/32	0.885	0.945	0.982
23/32	0.824	0.904	0.959
24/32	0.749	0.845	0.915
25/32	0.663	0.768	0.853
26/32	0.567	0.653	0.741
27/32	0.462	0.563	0.668
28/32	0.352	0.443	0.550
29/32	0.246	0.319	0.421
30/32	0.142	0.186	0.271
31/32	0.055	0.069	0.110
1(A.P.)	0.004	0.005	0.010

TABLE 2: MODEL MERCHANT SHIP OBSERVATIONS

$$\text{Upper Entry} = \frac{P(1-\gamma^2)}{\frac{1}{2}\rho V^2}$$

$$\text{Lower Entry} = \frac{P(1-\gamma^2)}{\frac{1}{2}\rho V^2} \cdot \frac{L^3}{\nabla}$$

Ship	RIPON	KINTERBURY	BIRCHOL	SPA	
∇/L^3	8.38×10^{-3}	8.45×10^{-3}	8.91×10^{-3}	10.22×10^{-3}	Mean
h/L = 0.094	0.224 26.8	0.237 28.0		0.336 32.9	29.2
0.125	0.153 18.3	0.158 18.7	0.175 19.6	0.195 19.1	18.9
0.20	0.081 9.67	0.082 9.70	0.094 10.5	0.093 9.1	9.74
0.375	0.032 3.8	0.036 4.26		0.038 3.7	3.92
0.50	0.022 2.6	0.022 2.6		0.024 2.4	2.53
0.625	0.014 1.67	0.015 1.77		0.018 1.76	1.73

TABLE 3: DEPENDENCE OF P UPON γ - SERIES 60 SHIPS

h/L	γ	SHIP					
		C_P = 0.614		C_P = 0.710		C_P = 0.805	
0.1	0.1 0.4	0.165 0.182	1.1	0.181 0.202	1.115	0.231 0.259	1.12
0.2	0.1 0.4	0.0685 0.077	1.125	0.073 0.082	1.12	0.083 0.094	1.13
0.4	0.1 0.4	0.0215 0.025	1.16	0.0257 0.0297	1.16	0.0297 0.0339	1.14
0.8	0.1 0.4	0.0044 0.0054	1.23	0.0057 0.00695	1.22	0.00715 0.0087	1.22

Quantities tabulated:-

$\left(\frac{P}{\frac{1}{2}\rho V^2}\right)_{\gamma = 0.1}$ $\left(\frac{P}{\frac{1}{2}\rho V^2}\right)_{\gamma = 0.4}$	RATIO lower to upper entry entry

Conclude that the variation of P with γ does not depend on the shape of the ship but that it is slightly influenced by the ratio depth/length.

$$\text{Mean value of } \left(\frac{P}{\frac{1}{2}\rho V^2}\right)_{\gamma = 0.4} \Bigg/ \left(\frac{P}{\frac{1}{2}\rho V^2}\right)_{\gamma = 0.1} = 1.16$$

$$\text{Value of } \frac{(1-\gamma^2)_{\gamma = 0.1}}{(1-\gamma^2)_{\gamma = 0.4}} = 1.18$$

- shows general consistency with a $(1-\gamma^2)^1$ law.

TABLE 4: SERIES 60 SHIPS

VALUE OF $C_p \cdot \dfrac{P(1-\gamma^2)}{\frac{1}{2}\rho V^2} \cdot \dfrac{L^3}{\nabla}$

h/L	C_P = 0.614	C_P = 0.710	C_P = 0.805
0.1	22.0	21.9	23.1
0.2	9.3	8.52	8.34
0.4	3.03	3.11	3.02
0.8	0.65	0.72	0.77

--- TABLE 5 OPPOSITE ---

TABLE 6: COMPARISON OF DETAILED AND APPROXIMATE ESTIMATES OF θ/θ_L

Ship	C_P	γ	h/L	(θ/θ_L) Detailed	(θ/θ_L) Approx.
Series 60	0.614	0.4	0.4	0.878	0.868
Series 60	0.614	0.4	0.2	0.735	0.755
Series 60	0.805	0.4	0.4	0.984	0.993
Series 60	0.710	0.4	0.1	0.781	0.708
ROWALLAN CASTLE	0.65	0.27	0.171	0.74	0.77
WATERLAND	0.73		0.391	0.94	0.98

TABLE 5: VARIATION OF DIMENSIONLESS $P\theta^2$ WITH

(1)	(2)	(3)	(4)	(5)	
Ship	$\frac{h}{L}$	γ	$\frac{P}{\frac{1}{2}\rho V^2}$	$\left(\frac{\theta}{\theta_L}\right)^2$	$\frac{P}{\frac{1}{2}\rho V^2}\left(\frac{\theta}{\theta_L}\right.$
Series 60 $C_P = 0.614$ $\frac{\nabla}{L^3} = 4.27 \times 10^{-3}$	0.1	0.4	0.182	0.501	0.0835
		0.1	0.165	0.501	0.0823
	0.2	0.4	0.0770	0.540	0.0381
		0.1	0.0688	0.559	0.0383
	0.4	0.4	0.0252	0.771	0.0178
		0.1	0.0215	0.824	0.0176
	0.8	0.4	0.00542	1.664	0.00826
		0.1	0.00440	1.877	0.00822
Series 60 $C_P = 0.710$ $\frac{\nabla}{L^3} = 5.72 \times 10^{-3}$	0.1	0.4	0.202	0.610	0.113
		0.1	0.181	0.610	0.110
	0.2	0.4	0.0815	0.650	0.0485
		0.1	0.0730	0.664	0.0483
	0.4	0.4	0.0298	0.850	0.0232
		0.1	0.0257	0.907	0.0232
	0.8	0.4	0.00695	1.740	0.0111
		0.1	0.00568	1.965	0.0111
Series 60 $C_P = 0.805$ $\frac{\nabla}{L^3} = 7.57 \times 10^{-3}$	0.1	0.4	0.259	0.736	0.175
		0.1	0.231	0.736	0.169
	0.2	0.4	0.0936	0.767	0.0658
		0.1	0.0825	0.778	0.0639
	0.4	0.4	0.339	0.968	0.0300
		0.1	0.297	1.020	0.0301
	0.8	0.4	0.00869	1.850	0.0147
		0.1	0.00715	2.068	0.0147
SPA $C_P = 0.768$ $\frac{\nabla}{L^3} = 10.22 \times 10^{-3}$	0.094	0.4	0.368	0.685	0.231
	0.125	0.4	0.250	0.691	0.158
	0.25	0.4	0.0958	0.748	0.0656
	0.375	0.4	0.0539	0.880	0.0434
	0.50	0.4	0.0328	1.077	0.0324
	0.625	0.4	0.0210	1.336	0.0257
	0.75	0.4	0.0140	1.633	0.0209

ENSIONLESS $P\theta^2$ WITH h/L - KEEL-LINE VALUES

(5)	(6)	(7)	(8)
$\left(\frac{\theta}{\theta_L}\right)^2$	$\frac{P}{\frac{1}{2}\rho V^2}\left(\frac{\theta}{\theta_L}\right)^2 (1-\gamma^2)^{\frac{1}{2}}$	$\frac{P}{\frac{1}{2}\rho V^2}\left(\frac{\theta}{\theta_L}\right)^2 (1-\gamma^2)^{\frac{1}{2}} \frac{L^3}{\nabla}$	$\frac{P}{\frac{1}{2}\rho V^2}\left(\frac{\theta}{\theta_L}\right)^2 (1-\gamma^2)^{\frac{1}{2}} \frac{L^3}{\nabla} \frac{h}{L}^{1.08}$
.501 .501	0.0835 (829) 0.0823	19.4	1.61
.540 .559	0.0381 (382) 0.0383	8.91	1.56
.771 .824	0.0178 (177) 0.0176	4.15	1.54
.664 .877	0.00826 (824) 0.00822	1.94	1.52
.610 .610	0.113 (112) 0.110	19.4 (18.1)	1.61 (1.50)
.650 .664	0.0485 (484) 0.0483	8.42	1.48
.850 .907	0.0232 (232) 0.0232	4.05	1.51
.740 .965	0.0111 (111) 0.0111	1.94	1.52
.736 .736	0.175 (172) 0.169	22.7 (18.9)	1.88 (1.57)
.767 .778	0.0658 (649) 0.0639	8.58	1.50
.968 .020	0.0300 (300) 0.0301	3.97	1.48
.850 .068	0.0147 (147) 0.0147	1.94	1.52
.685	0.231	22.60 (19.7)	1.75 (1.52)
.691	0.158	15.45 (14.0)	1.63 (1.48)
.748	0.0656	6.40	1.43
.880	0.0434	4.24	1.47
.077	0.0324	3.16	1.50
.336	0.0257	2.51	1.50
.633	0.0209	2.04	1.49
			Mean 1.51

TABLE 7: COMPARISON OF DETAILED AND APPROXIMATE ESTIMATES OF $\frac{P(1-\gamma^2)}{\frac{1}{2}\rho V^2}$

	$\frac{\lambda}{L}$	$\frac{P(1-\gamma^2)}{\frac{1}{2}\rho V^2}$ Detailed Theory	$\frac{P(1-\gamma^2)}{\frac{1}{2}\rho V^2}$ Simple Theory	Discrepancy
Series 60 C_P = 0.614				
0.1	0	0.182	0.172	$-5\frac{1}{2}$%
0.1	0.2	0.111	0.120	+8%
0.1	0.4	0.060	0.064	+7%
0.1	0.8	0.0224	0.0221	$-1\frac{1}{2}$%
0.2	0	0.077	0.086	$+11\frac{1}{2}$%
0.2	0.2	0.054	0.060	+11%
0.2	0.4	0.030	0.032	+7%
0.2	0.8	0.0112	0.0111	-1%
0.4	0	0.025	0.043	+72%
0.4	0.2	0.021	0.030	+43%
0.4	0.4	0.0137	0.0160	+17%
0.4	0.8	0.00555	0.00552	0%
0.8	0	0.0054	0.0215	+300%
0.8	0.2	0.00505	0.015	+200%
0.8	0.4	0.00415	0.00800	+100%
0.8	0.8	0.00237	0.00275	+16%
Series 60 C_P = 0.805				
0.1	0	0.171 0.259*	0.177	$+3\frac{1}{2}$%
0.1	0.2	0.135 0.137*	0.142	+5%
0.1	0.4	0.0873	0.089	+2%
0.1	0.8	0.0370	0.0357	$-3\frac{1}{2}$%
0.2	0	0.083 0.0936*	0.0885	+7%
0.2	0.2	0.0674	0.071	+5%
0.2	0.4	0.0436	0.044	+1%
0.2	0.8	0.0185	0.0179	$-3\frac{1}{2}$%
0.4	0	0.0339	0.0443	+28%
0.4	0.2	0.0292	0.0355	+22%
0.4	0.4	0.0206	0.0223	+8%
0.4	0.8	0.00922	0.00893	-3%
0.8	0	0.00869	0.0222	+160%
0.8	0.2	0.00814	0.0178	+120%
0.8	0.4	0.00681	0.0111	+63%
0.8	0.8	0.00400	0.00446	+12%

* Double-humped signatures - Mid-point value entered alongside. Agreement with the mid-point value would be expected.

) AND APPROXIMATE ESTIMATES OF $\frac{P(1-\gamma^2)}{\frac{1}{2}\rho V^2}$

$\frac{P(1-\gamma^2)}{\frac{1}{2}\rho V^2}$ Simple Theory	Discrepancy	$\frac{y^2}{L^2} - \frac{2h^2}{L^2} + \frac{Cp^2}{4}$
0.172	$-5\frac{1}{2}$%	+0.074
0.120	+8%	+0.114
0.064	+7%	+0.234
0.0221	$-1\frac{1}{2}$%	+0.714
0.086	$+11\frac{1}{2}$%	+0.0144
0.060	+11%	+0.0544
0.032	+7%	+0.174
0.0111	-1%	+0.654
0.043	+72%	-0.226
0.030	+43%	-0.186
0.0160	+17%	-0.066
0.00552	0%	+0.414
0.0215	+300%	-1.19
0.015	+200%	-1.15
0.00800	+100%	-1.03
0.00275	+16%	-0.546
0.177	$+3\frac{1}{2}$%	+0.142
0.142	+5%	+0.182
0.089	+2%	+0.302
0.0357	$-3\frac{1}{2}$%	+0.782
0.0885	+7%	+0.082
0.071	+5%	+0.122
0.044	+1%	+0.242
0.0179	$-3\frac{1}{2}$%	+0.722
0.0443	+28%	-0.158
0.0355	+22%	-0.118
0.0223	+8%	+0.002
0.00893	-3%	+0.642
0.0222	+160%	-1.12
0.0178	+120%	-1.08
0.0111	+63%	-0.958
0.00446	+12%	-0.478

s - Mid-point value entered alongside.
point value would be expected.

2

SERIES 60 SHIP $C_P = 0 \cdot 614$ KE

$\nabla / L^3 \quad 4 \cdot 27 \times 10^{-3}$

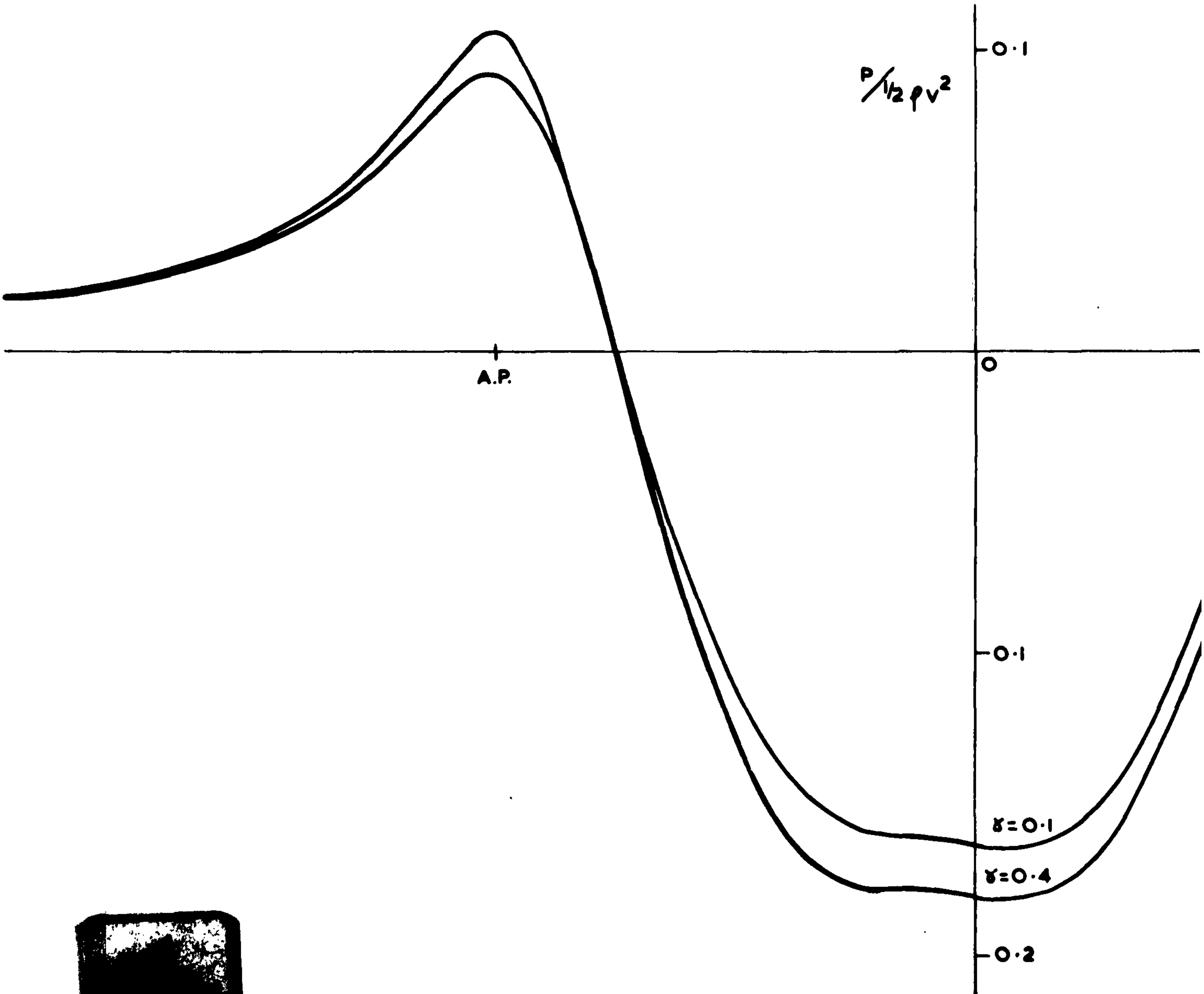

$C_p = 0.614$
$\nabla / L^3 \quad 4.27 \times 10^{-3}$

KEEL SIGNATURE
$\frac{h}{L} = 0.1$

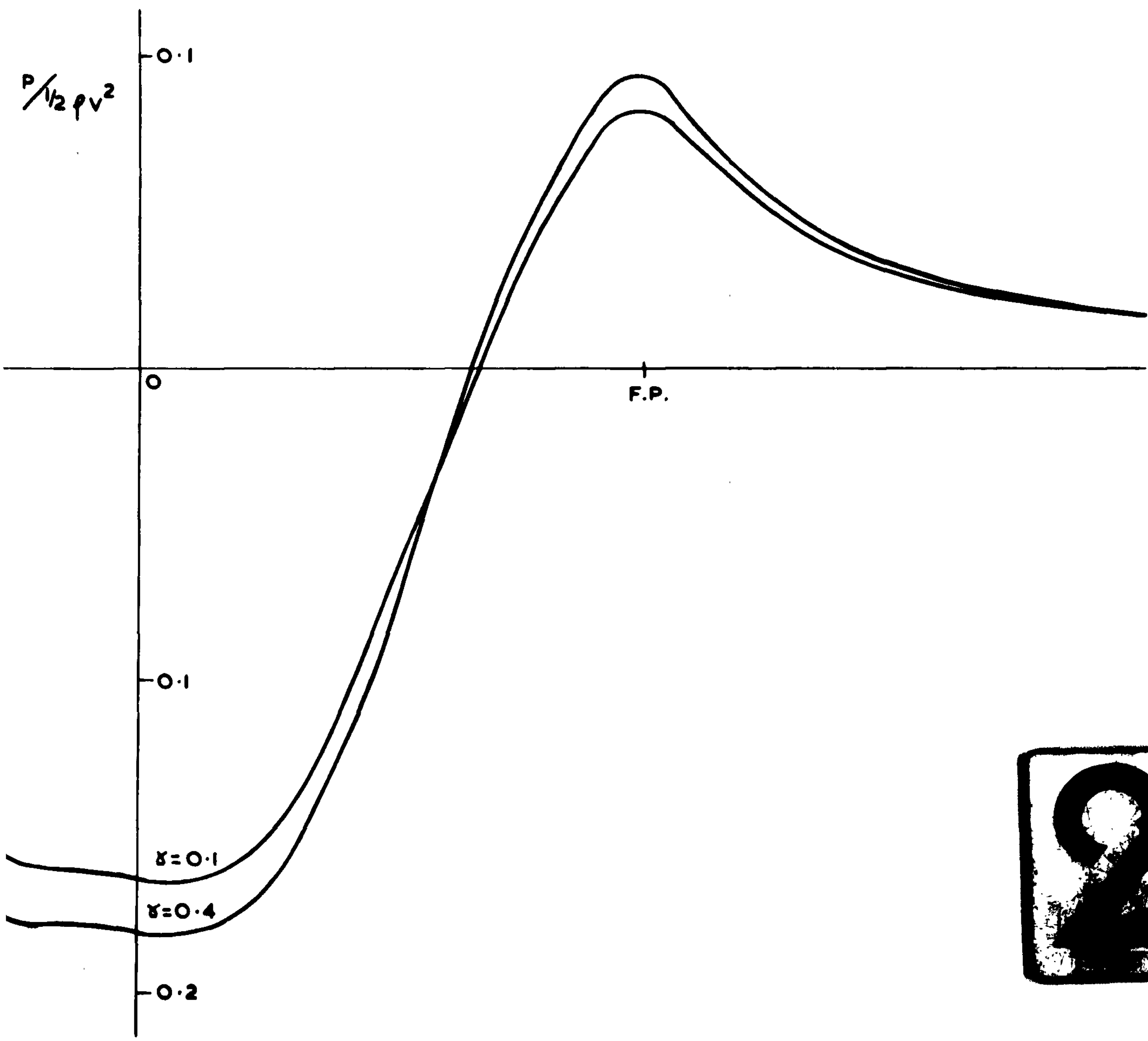

FIG. 1. SERIES 60 KEEL SIGNATURES.

SERIES 60 SHIP $C_p = 0{\cdot}614$

$\nabla / L^3 = 4{\cdot}27 \times 10^-$

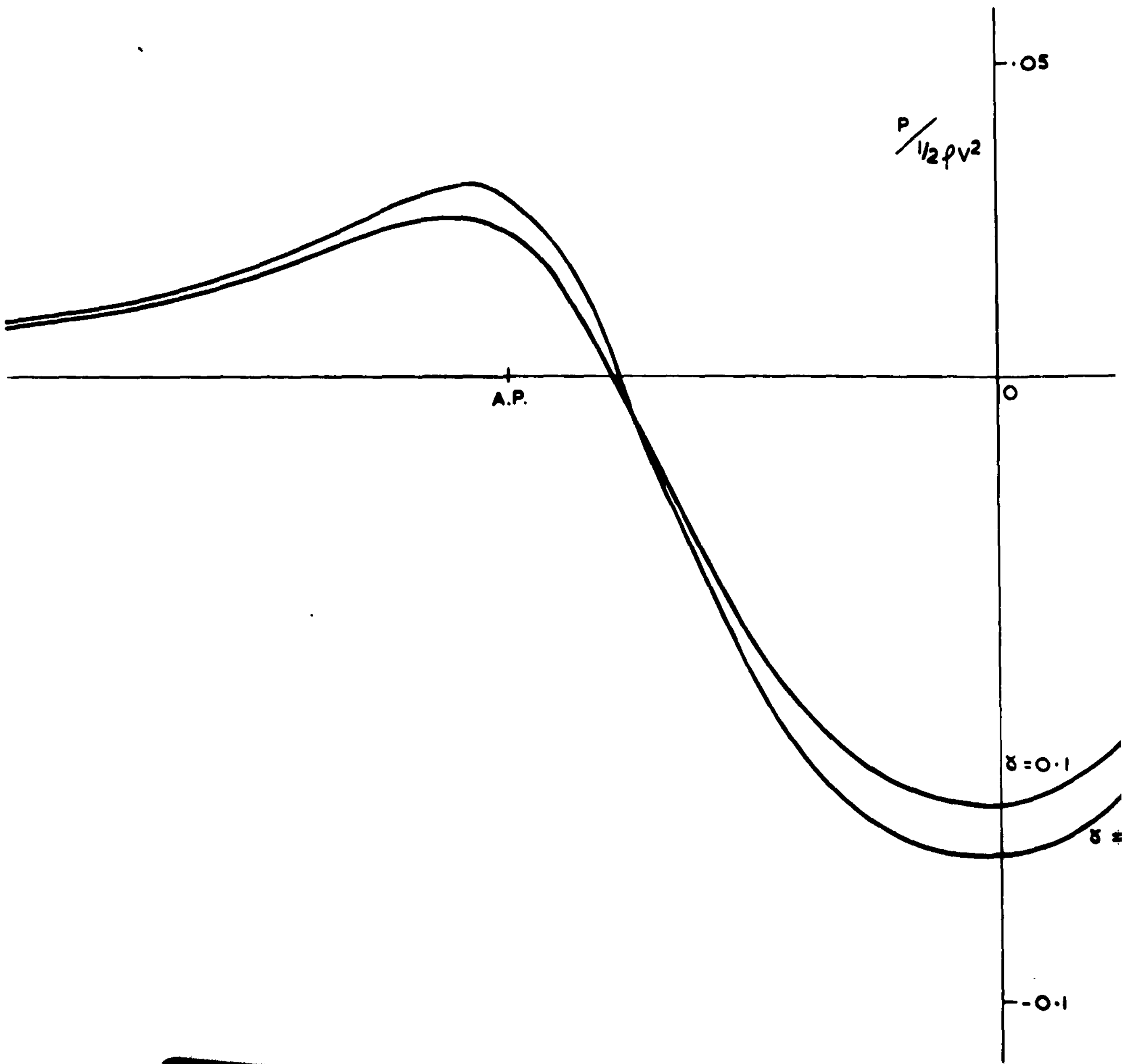

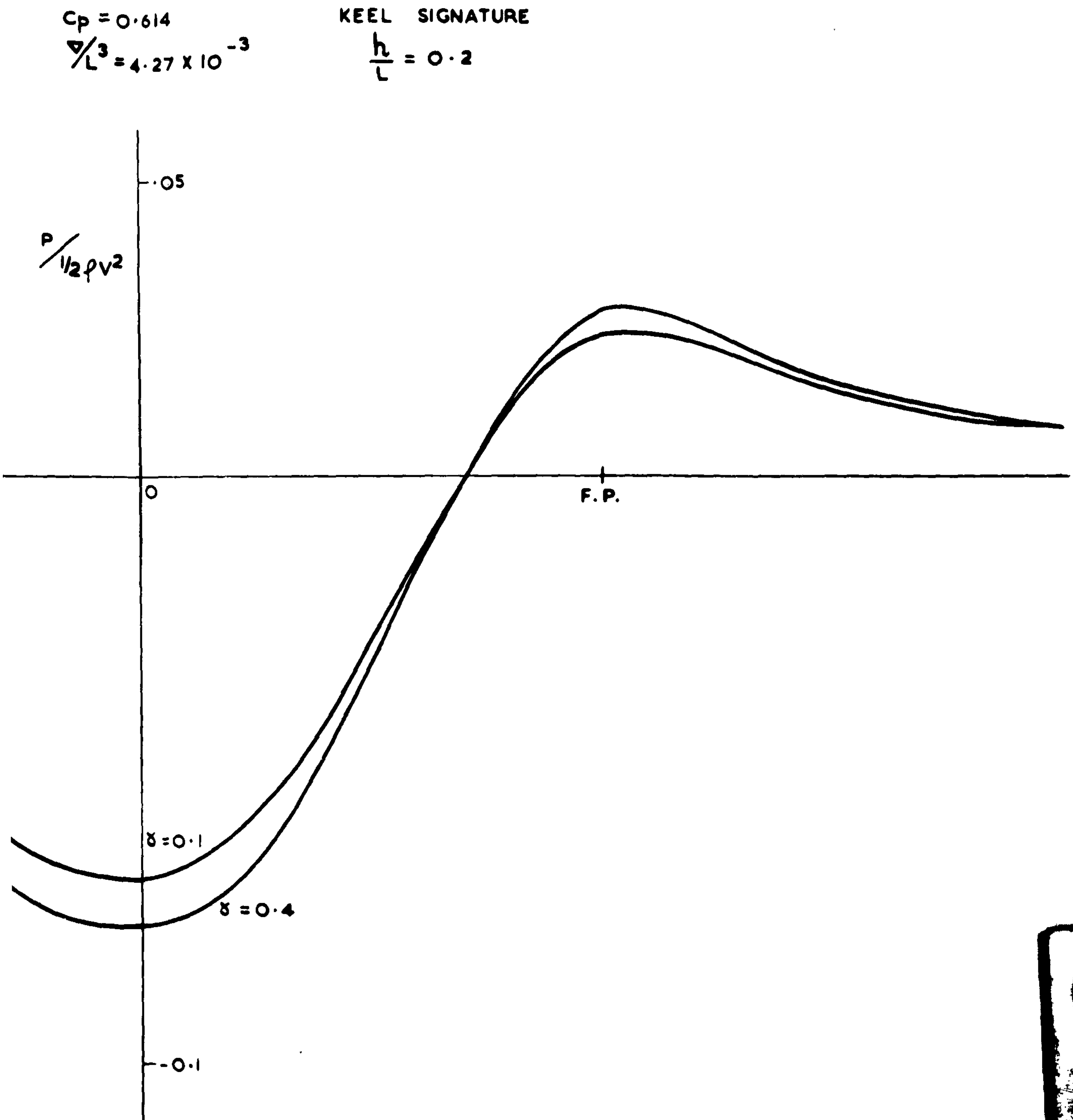

FIG. 2. SERIES 60 KEEL SIGNATURES.

SERIES 60 $C_p = 0.614$
$\nabla / L^3 = 4.27 \times 10^{-}$

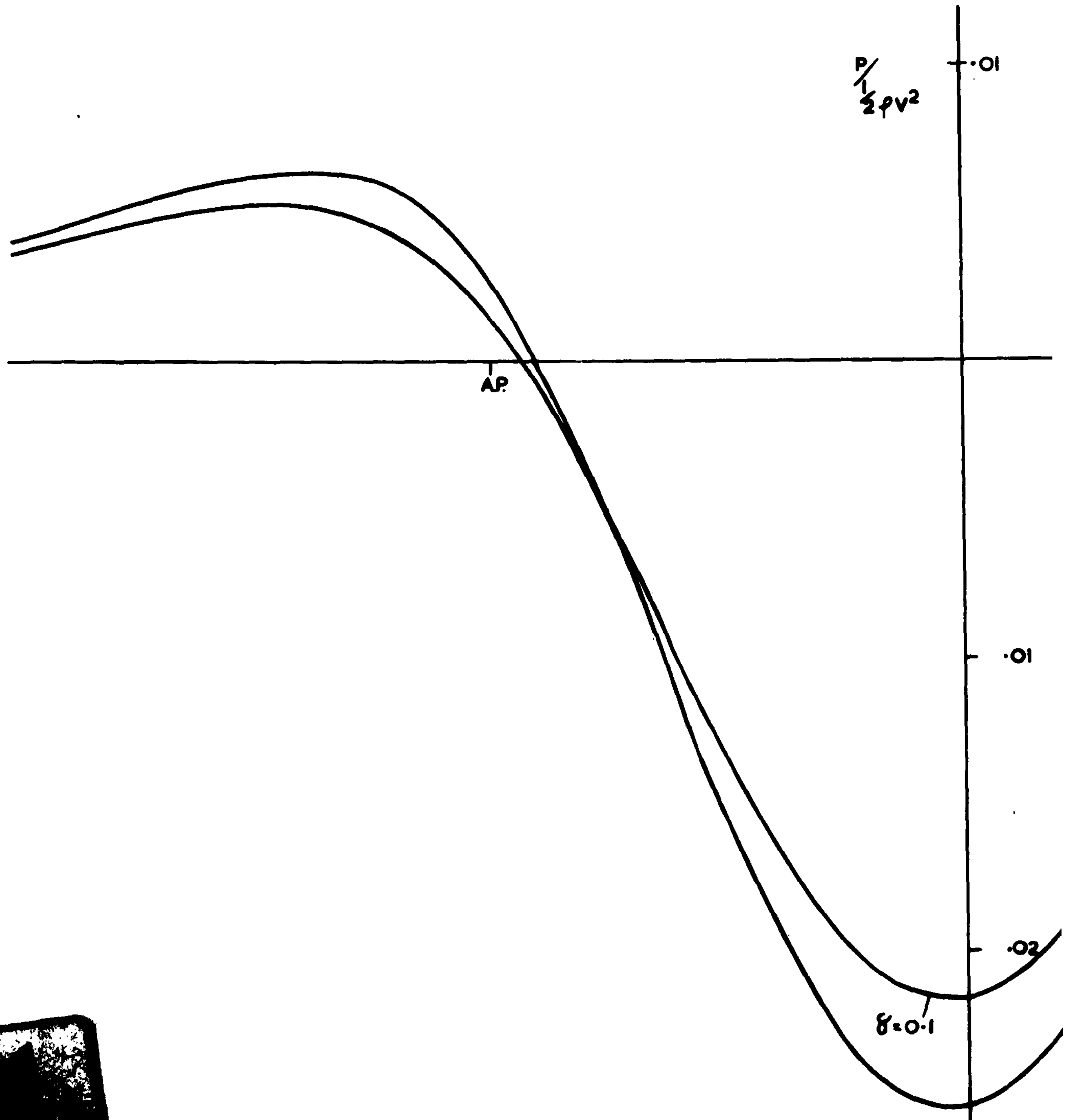

FIG. 3 SERIES 60 KEEL

O $C_p = 0.614$ KEEL SIGNATURE

$\nabla / L^3 = 4.27 \times 10^{-3}$ $h/L = 0.4$

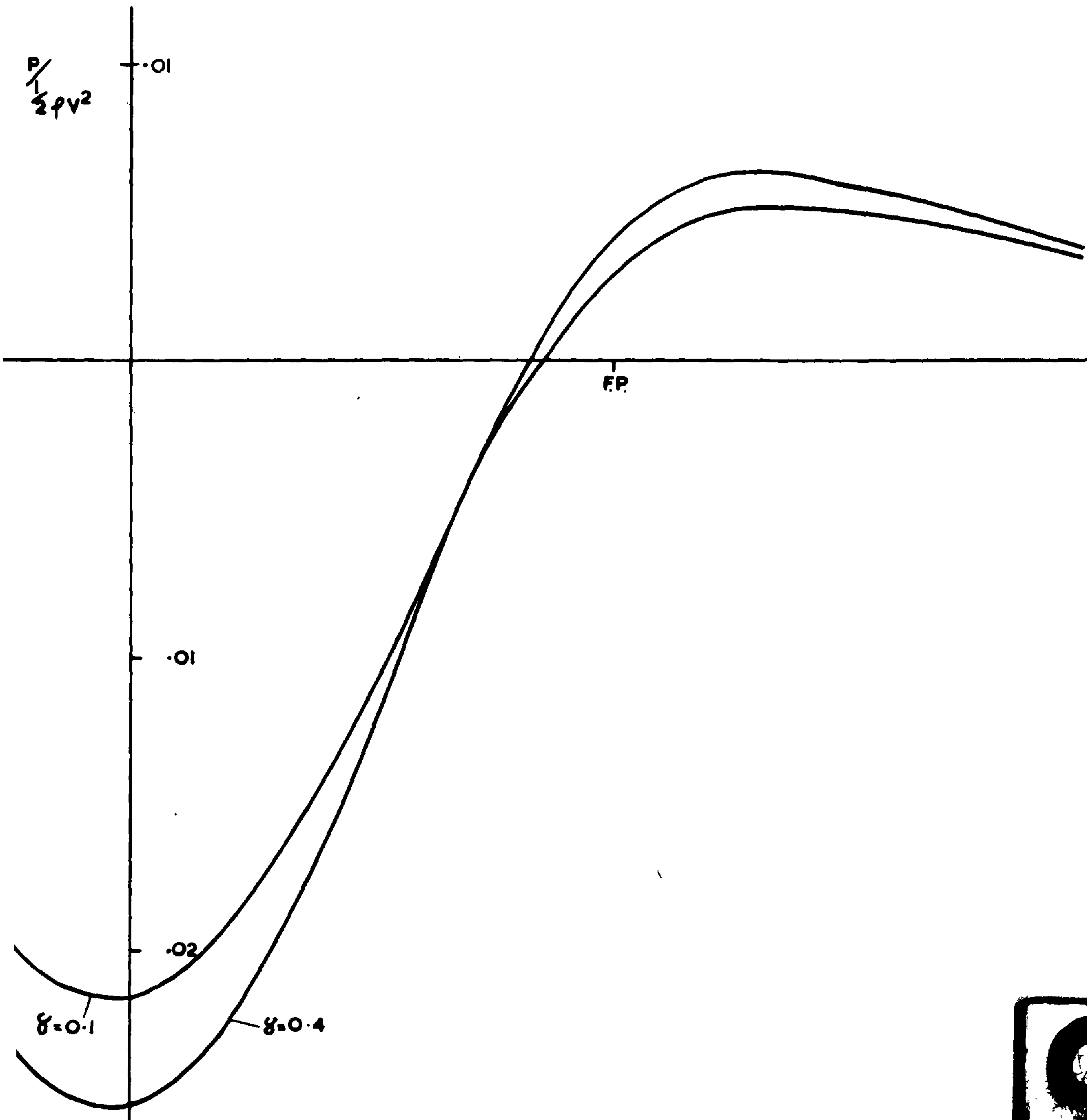

IES 60 KEEL SIGNATURES

SERIES 60 $C_p = 0{\cdot}614$

$\nabla/L^3 = 4{\cdot}27 \times 10$

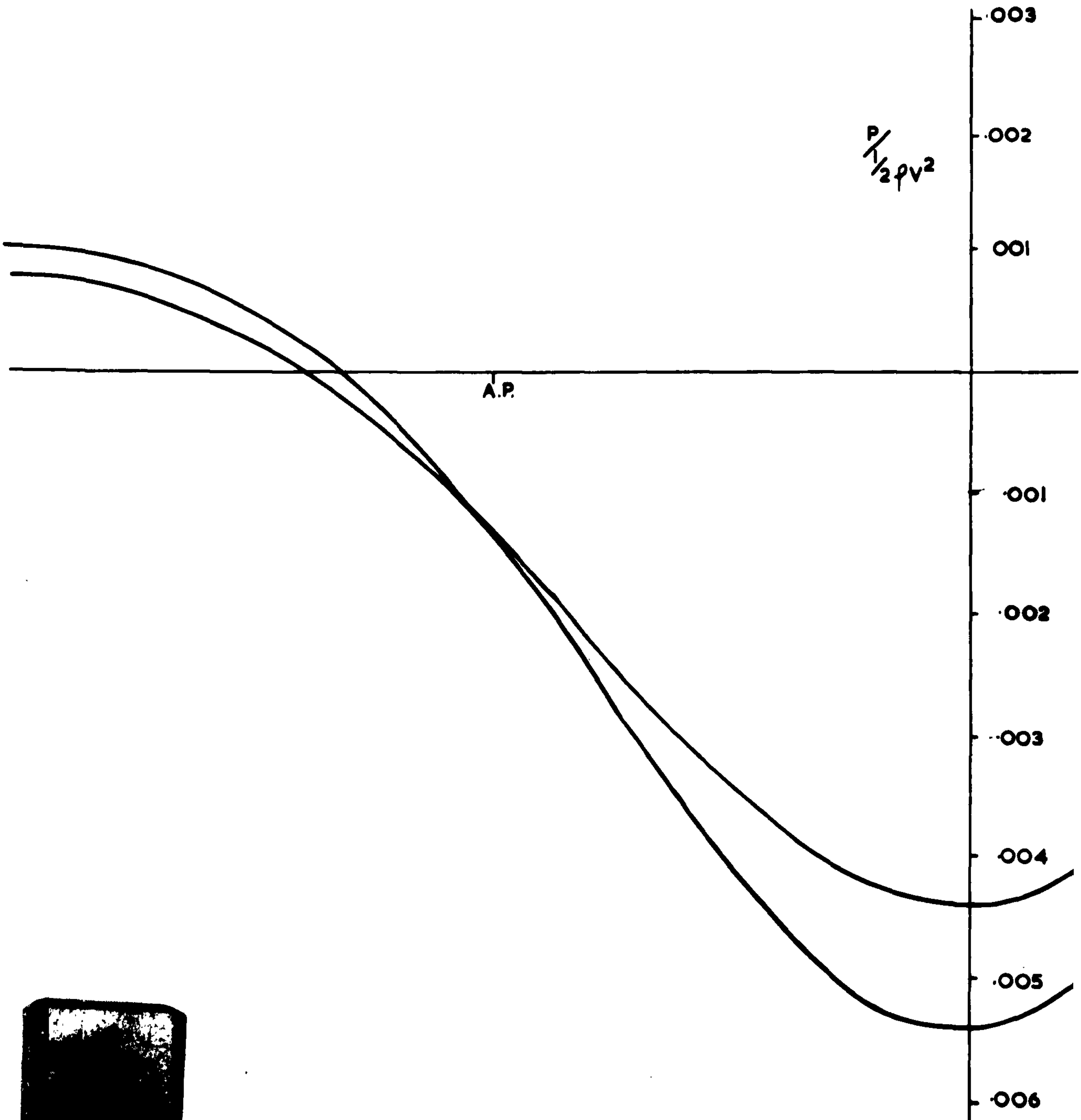

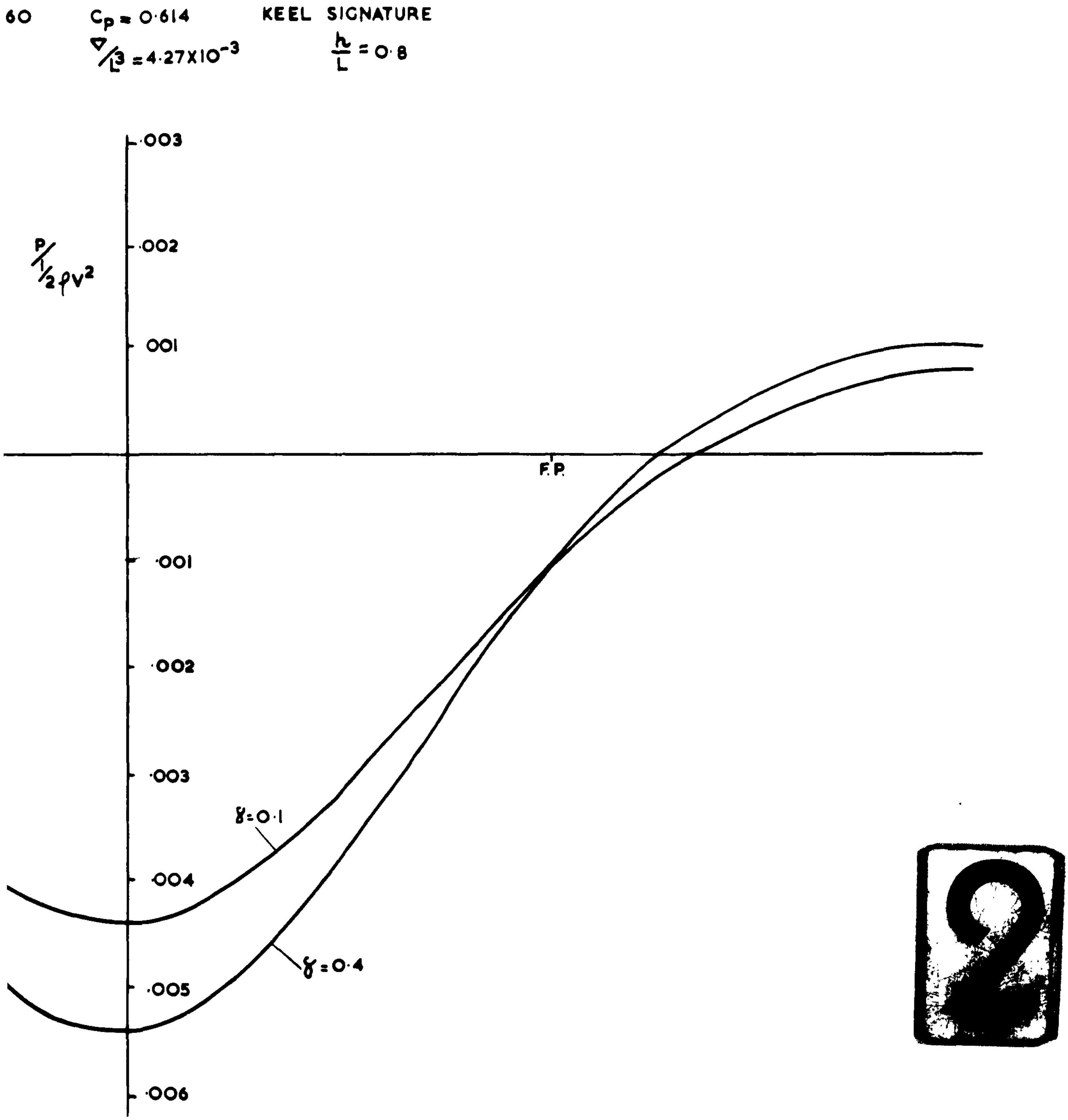

FIG. 4 SERIES 60 KEEL SIGNATURES

SERIES 60 SHIP $C_p = 0\cdot 710$

$\nabla/L^3 = 5\cdot 72 \times$

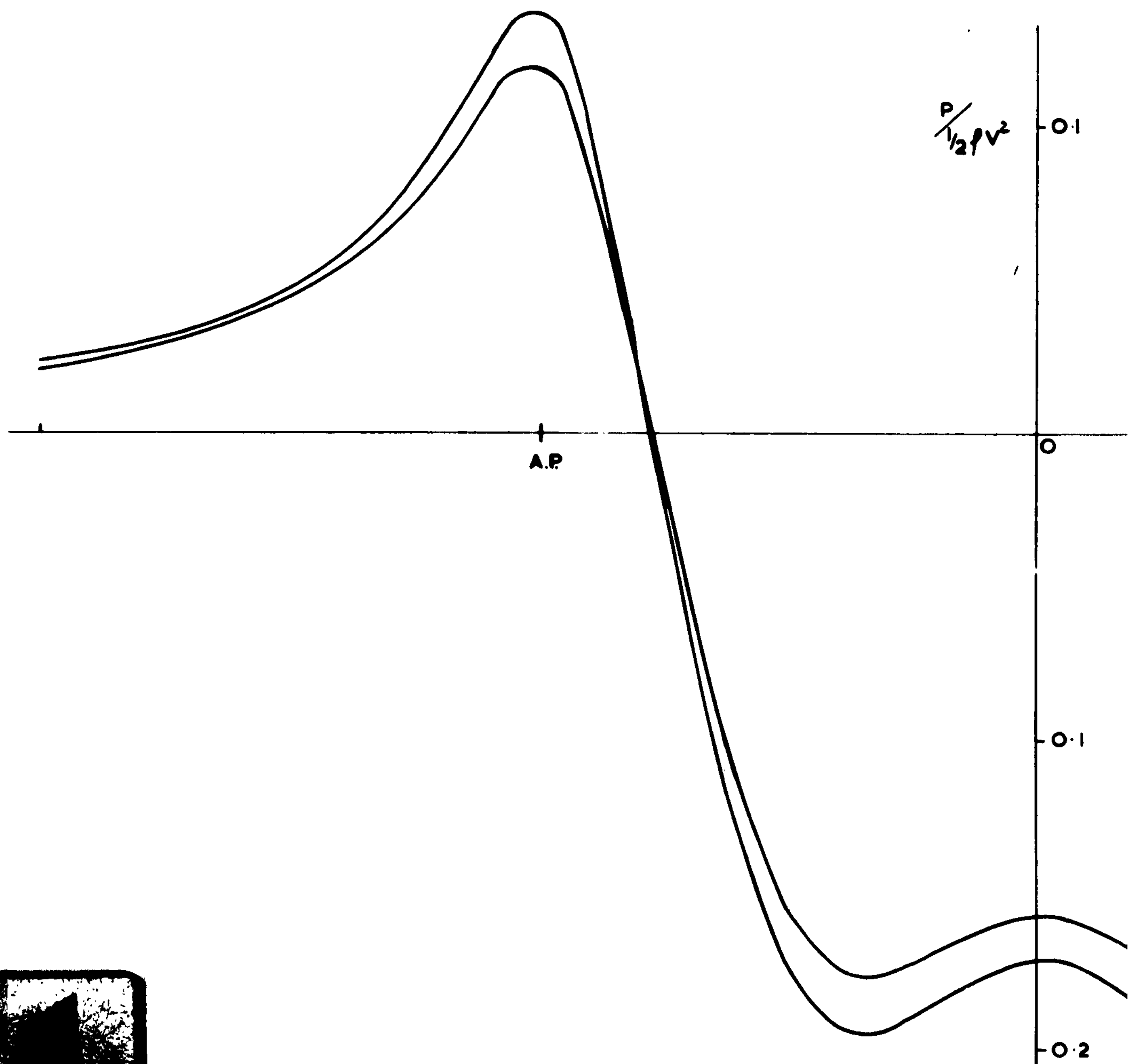

$C_p = 0 \cdot 710$ KEEL SIGNATURE

$\nabla / L^3 = 5 \cdot 72 \times 10^{-3}$ $\frac{h}{L} = 0 \cdot 1$

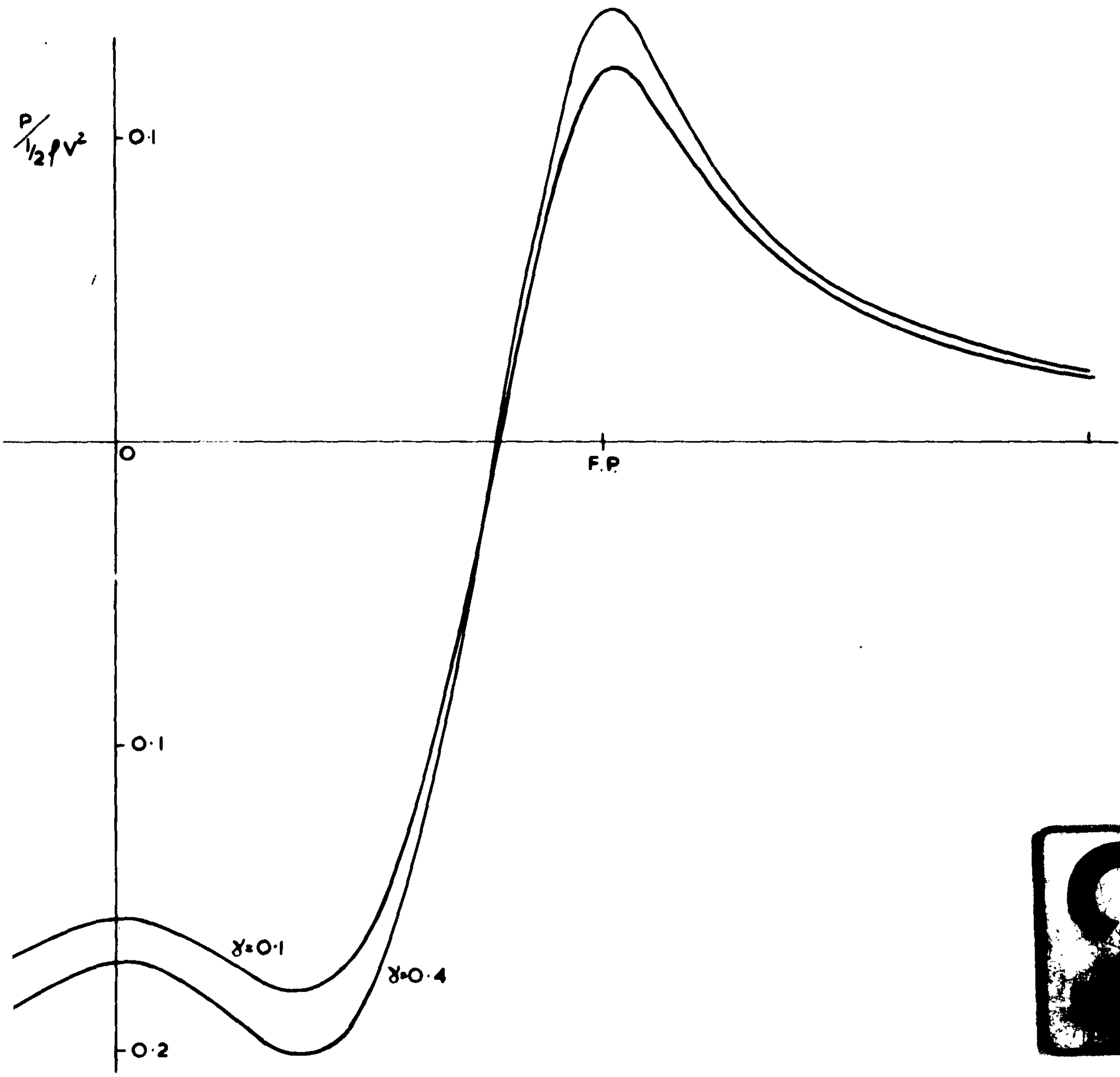

FIG. 5. SERIES 60 KEEL SIGNATURES.

SERIES 60 SHIPS $C_p = 0710$

$\nabla / L^3 = 5.72 \times 10$

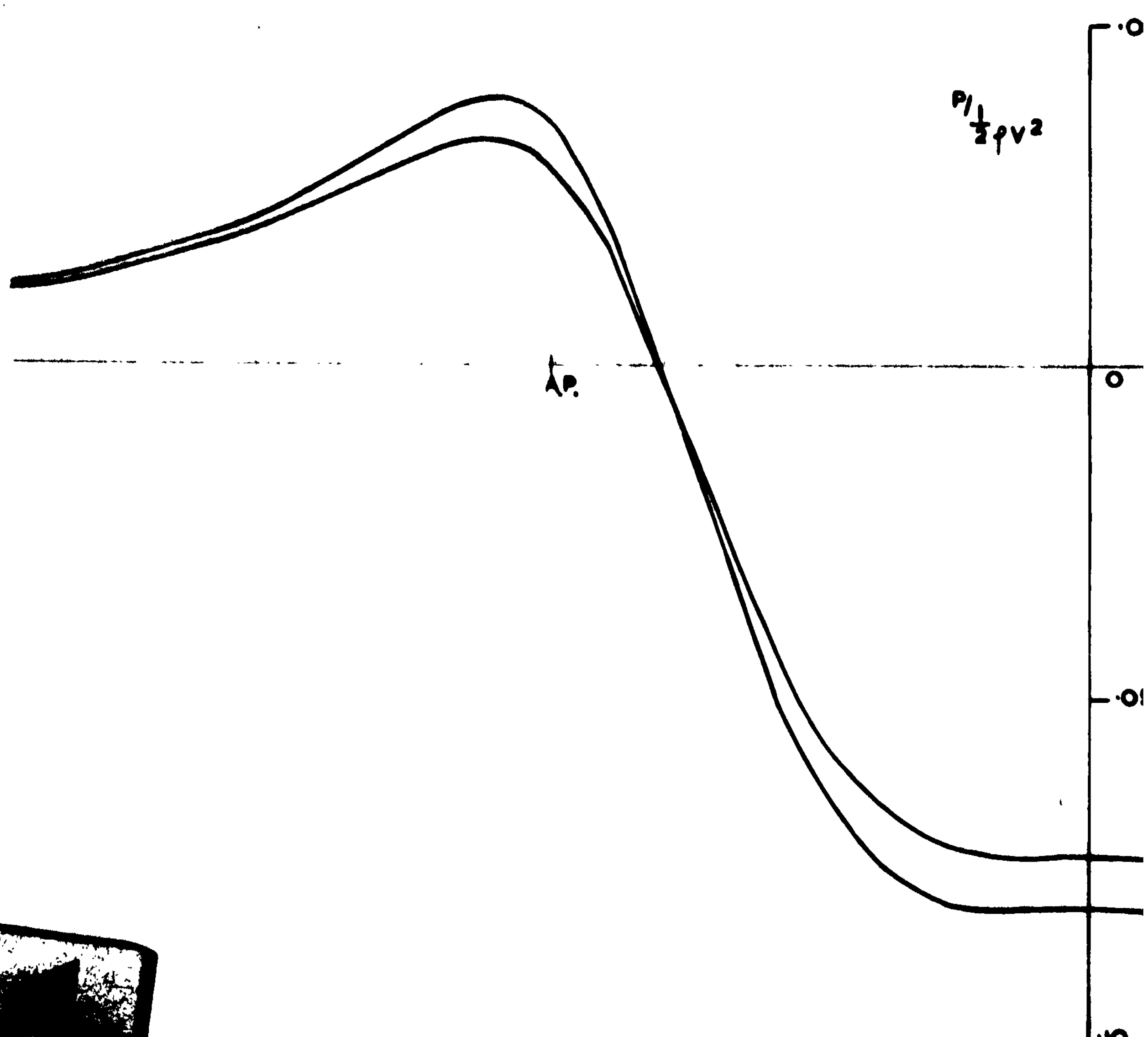

$C_p = 0710$ KEEL SIGNATURE

$\nabla/L^3 = 572 \times 10^{-3}$ $\quad \frac{h}{L} = 0.2$

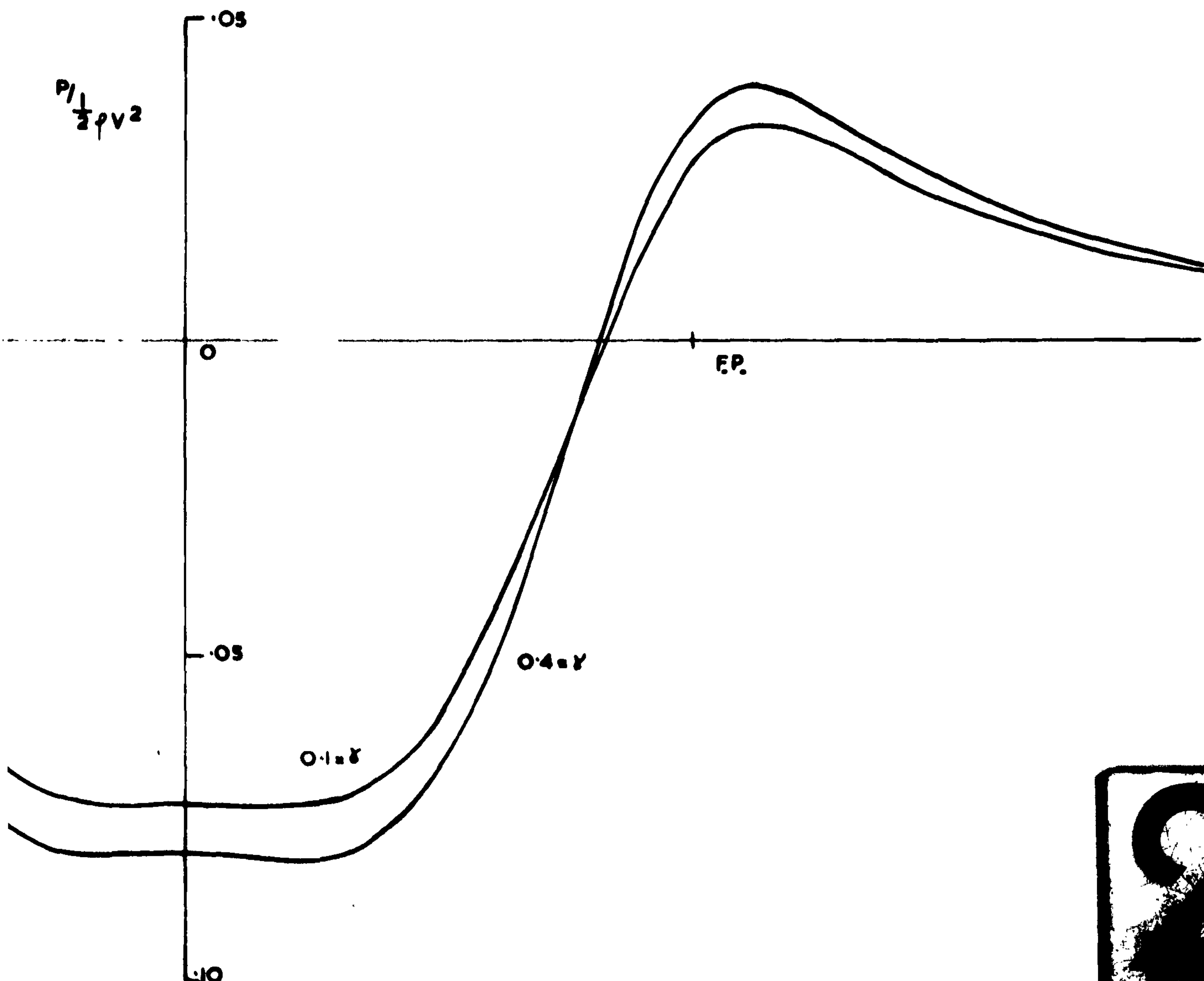

FIG.6 SERIES 60 KEEL SIGNATURES.

SERIES 60 SHIP Cp. = 0710 KI

$\nabla/L^3 = 5\ 72 \times 10^{-3}$ $\frac{h}{L}$

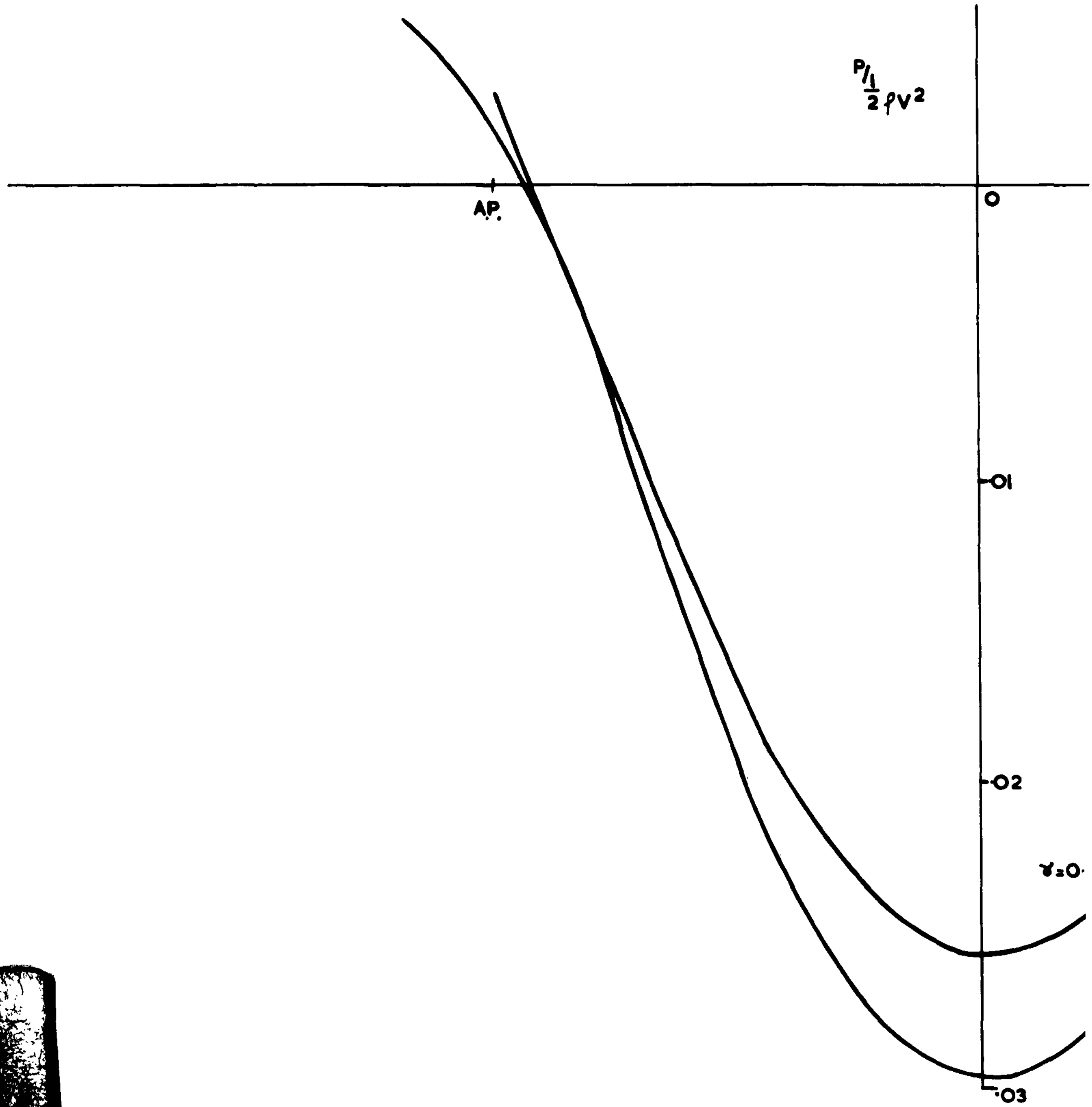

FIG.7 SERIES 60 KEEL SIGN

SERIES 60 SHIP $C_p = 0710$ KE

$\nabla / L^3 = 5\ 72 \times 10^{-3}$ $\frac{h}{L}$

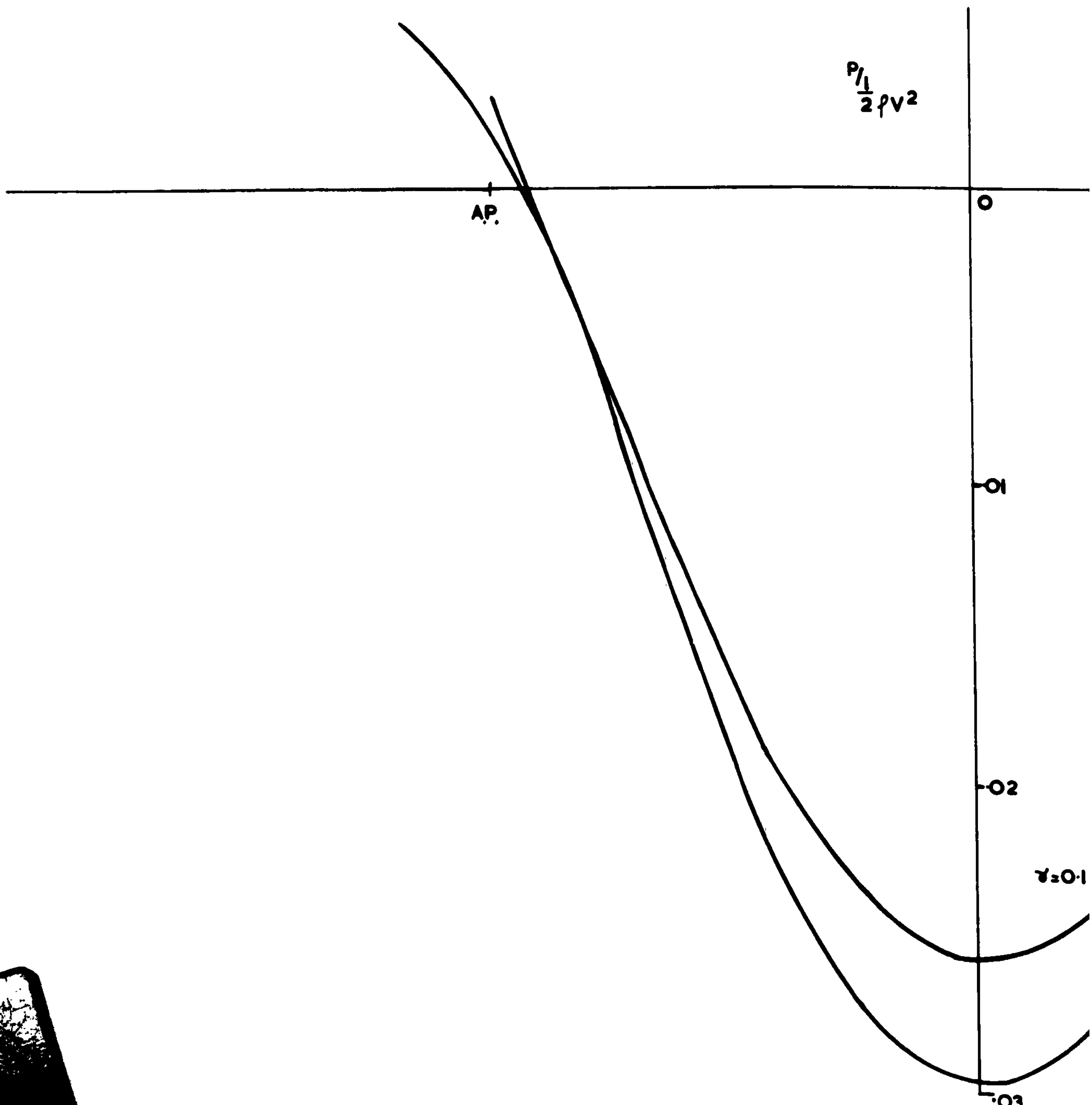

FIG.7 SERIES 60 KEEL SIGN

FIG.7.

: 0710 KEEL SIGNATURE

= 5 72x10^{-3} $\frac{h}{L}$ = 0·4

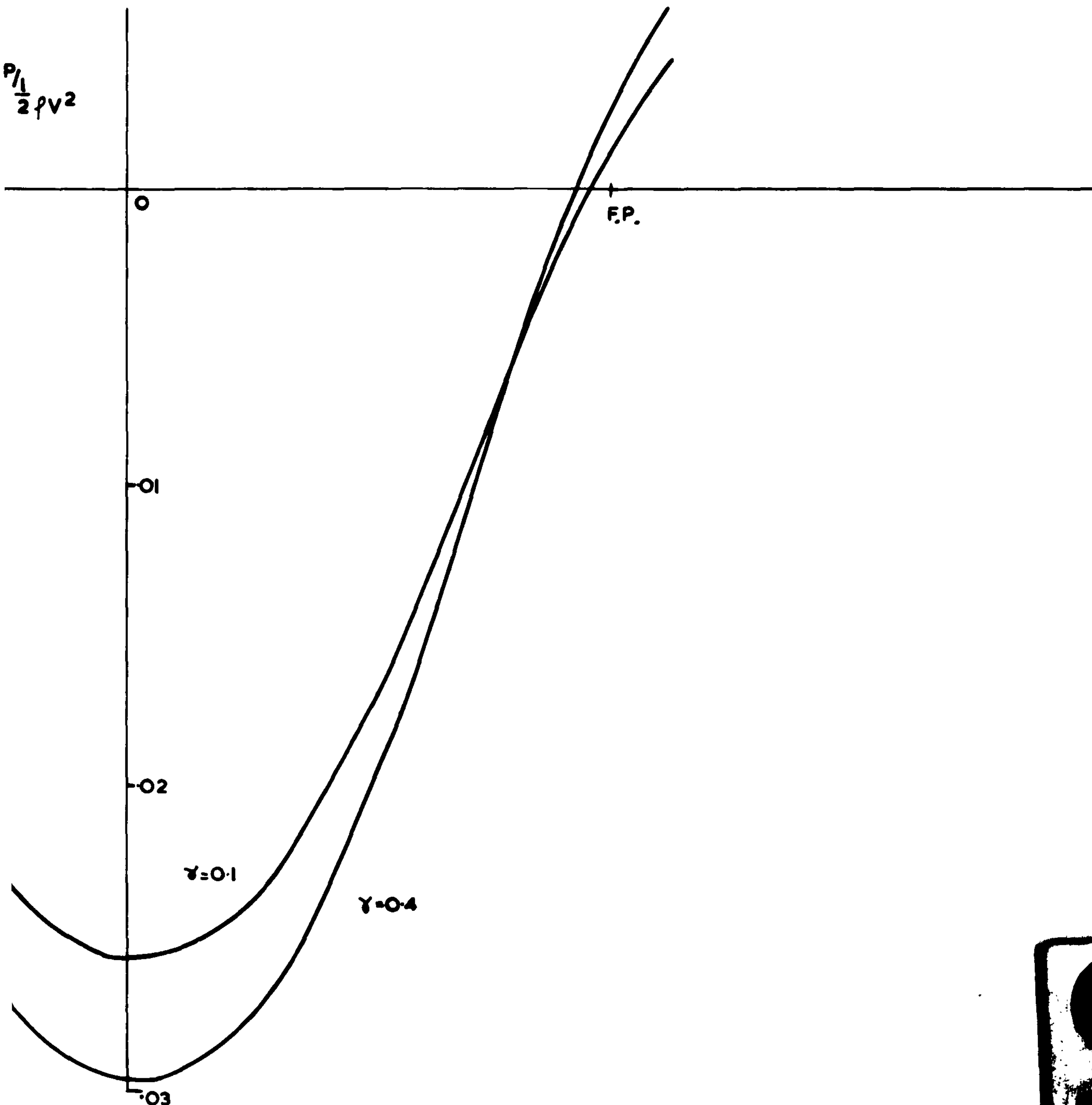

S 60 KEEL SIGNATURES.

SERIES 60 SHIP $C_p = 0.710$ $\nabla / L^3 = 5.72 \times 10$

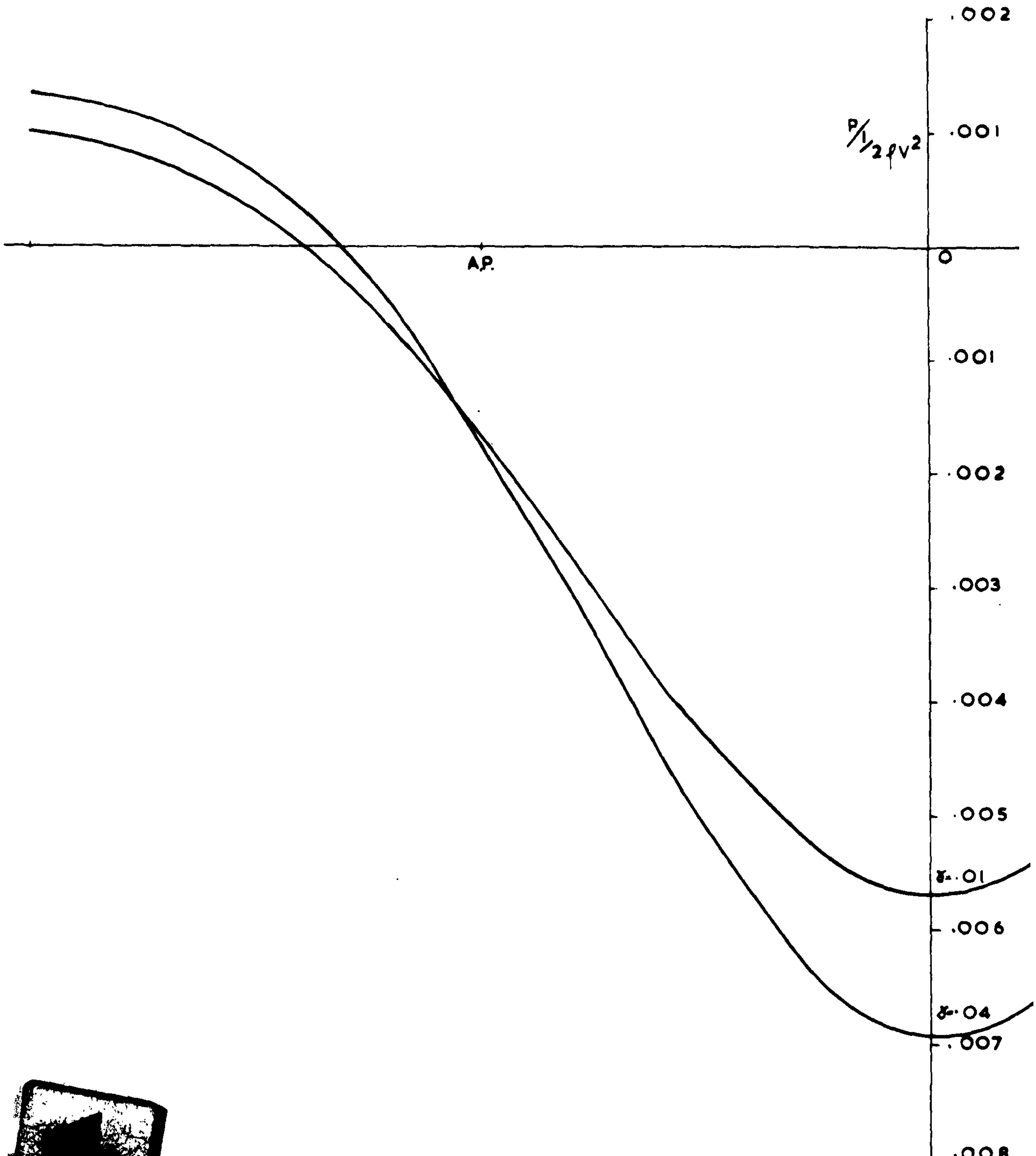

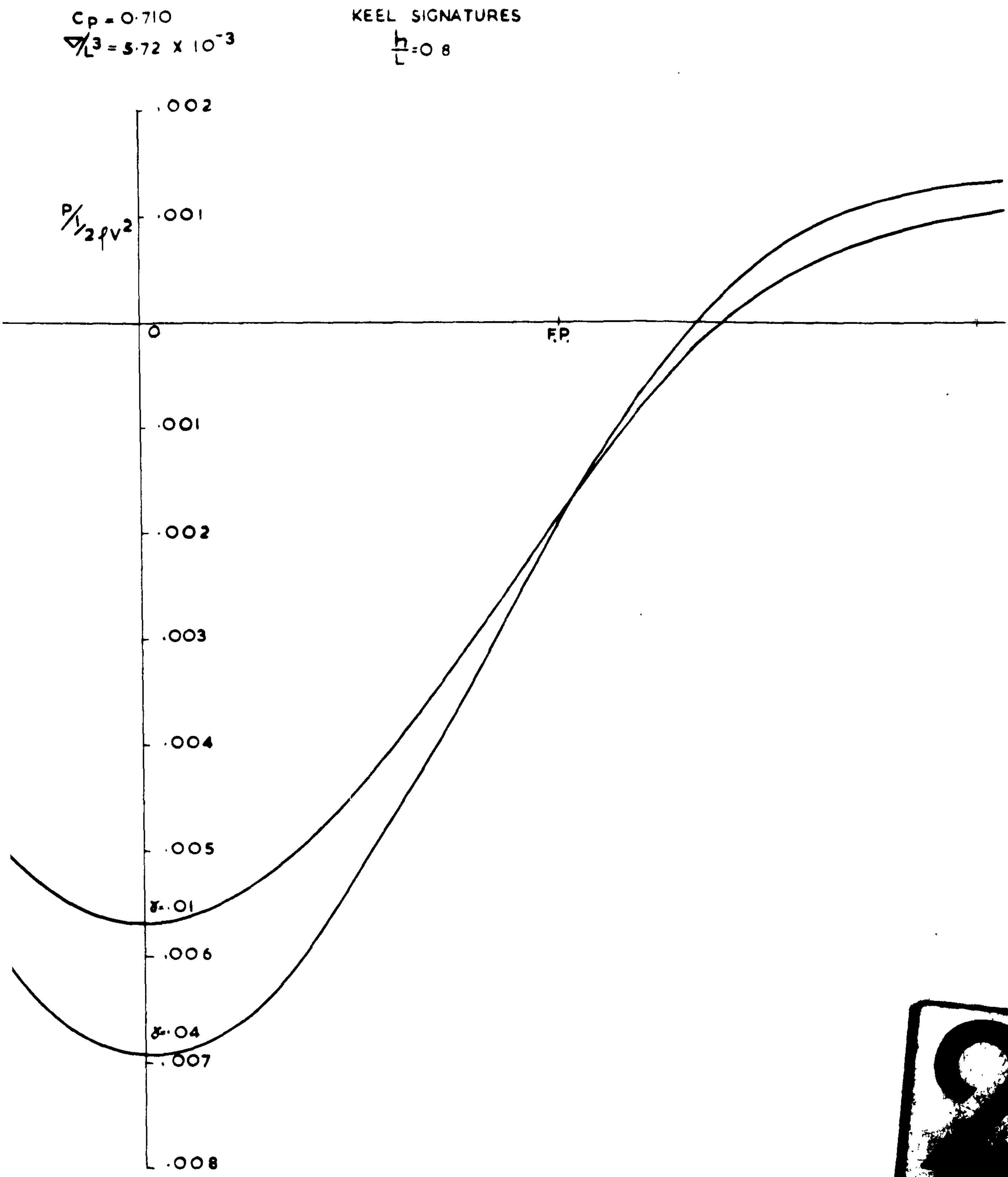

FIG.8.SERIES 60 KEEL SIGNATURES.

SERIES 60 SHIP

$C_p = 0.805$

$\nabla / L^3 = 7.57 \times 10^{-3}$

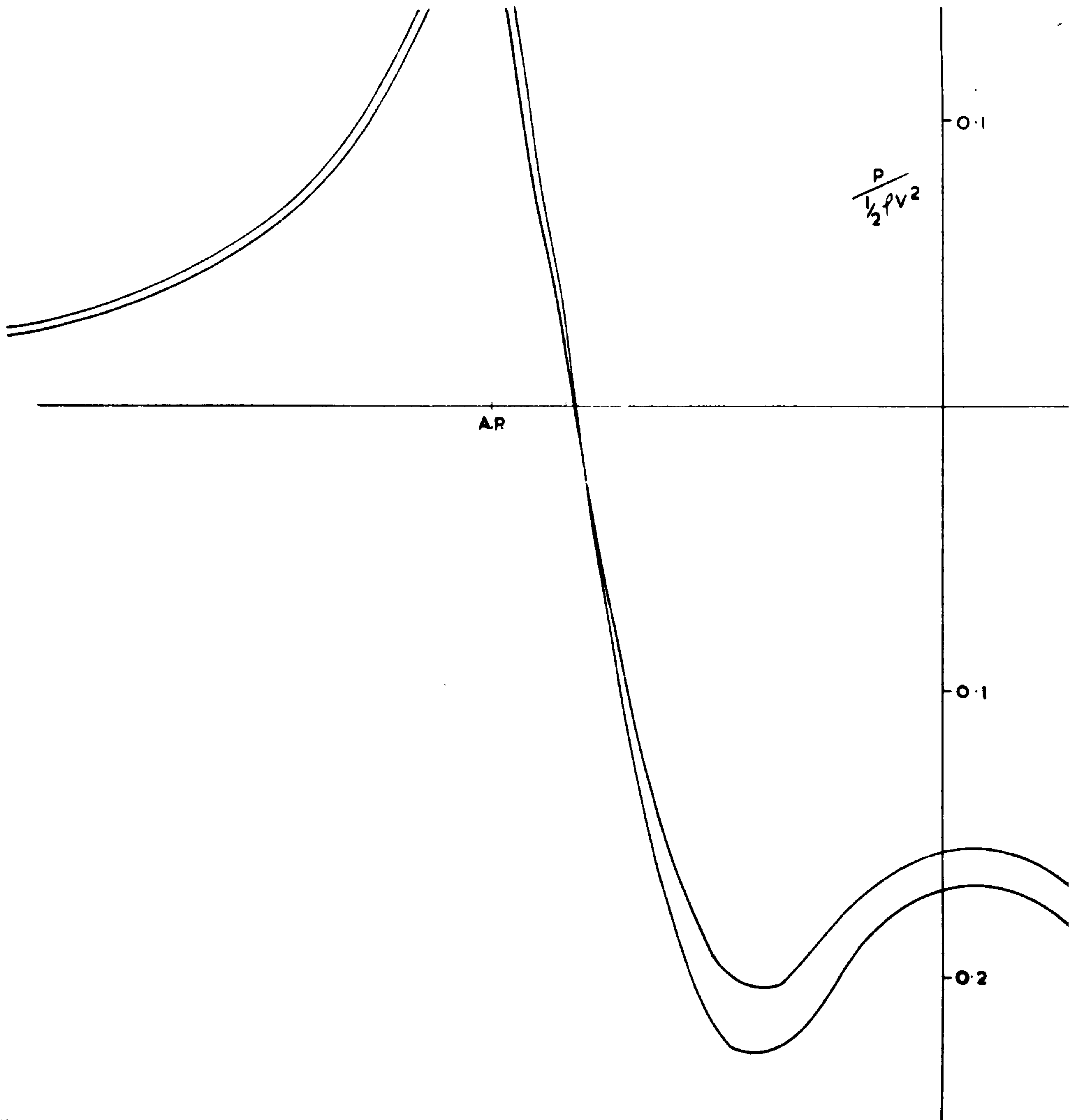

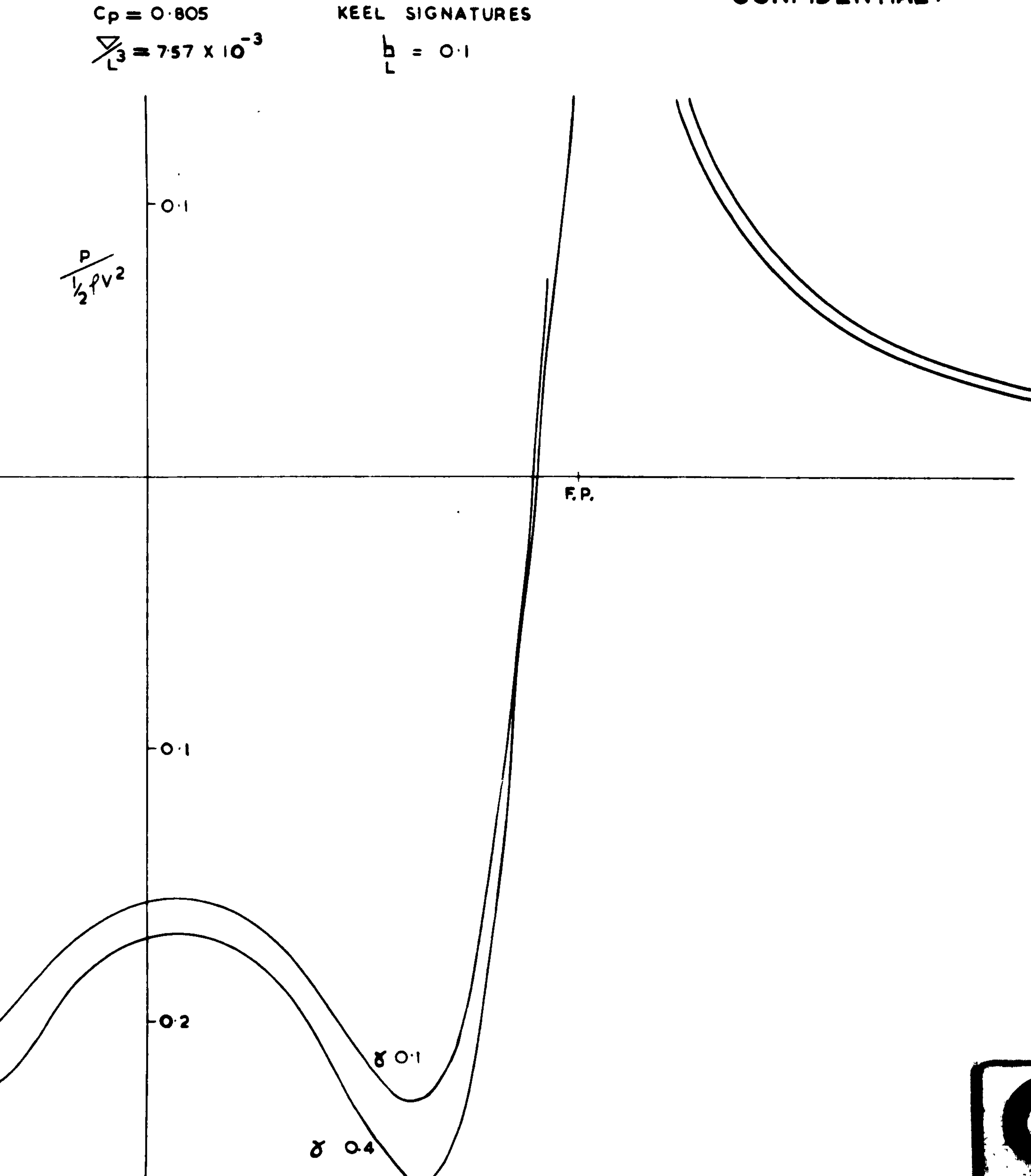

FIG.9 SERIES 60 KEEL SIGNATURES.
CONFIDENTIAL.

SERIES 60

$C_p = 0{\cdot}805$

$\nabla/L^3 = 7{\cdot}57 \times 10^{-3}$

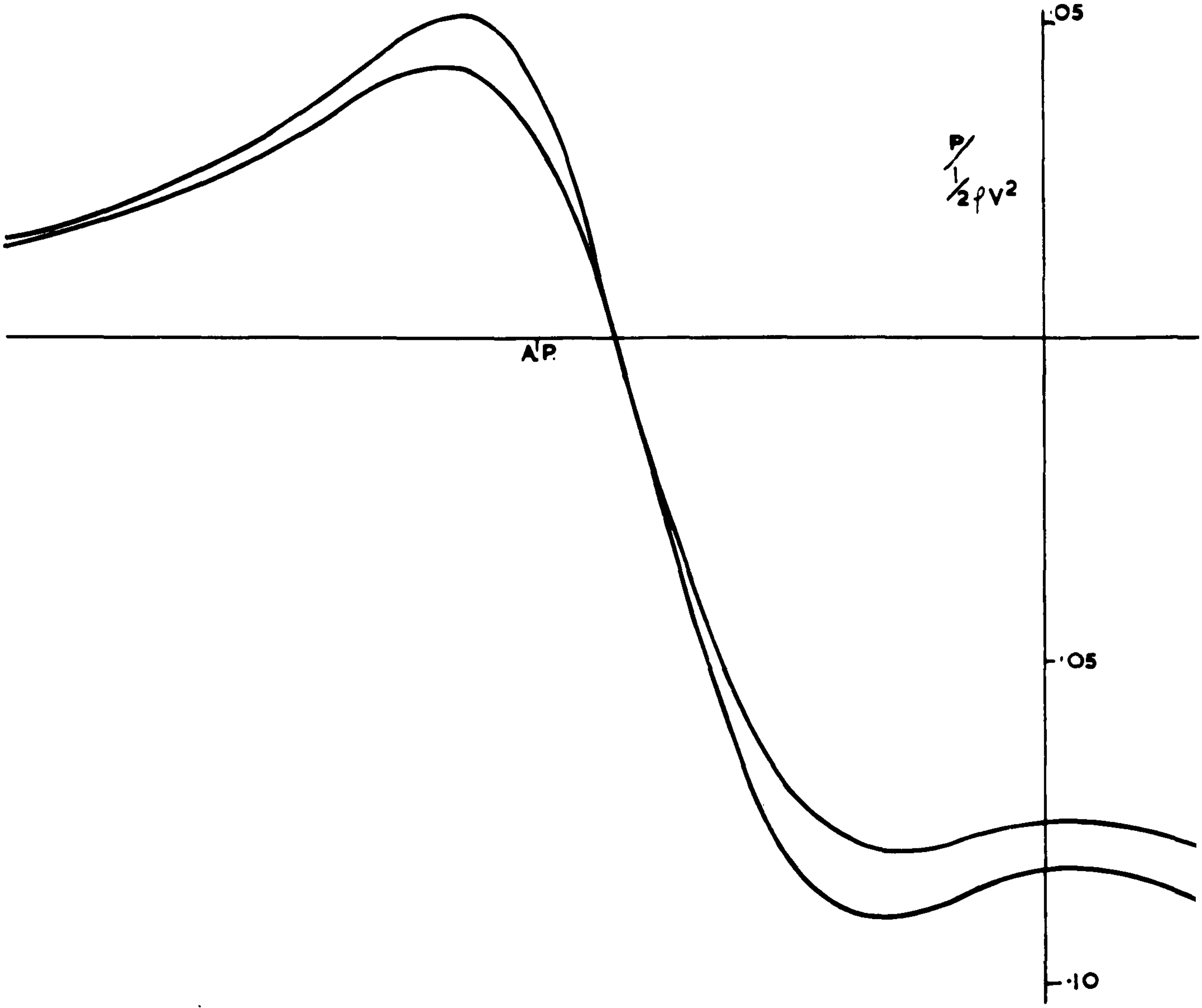

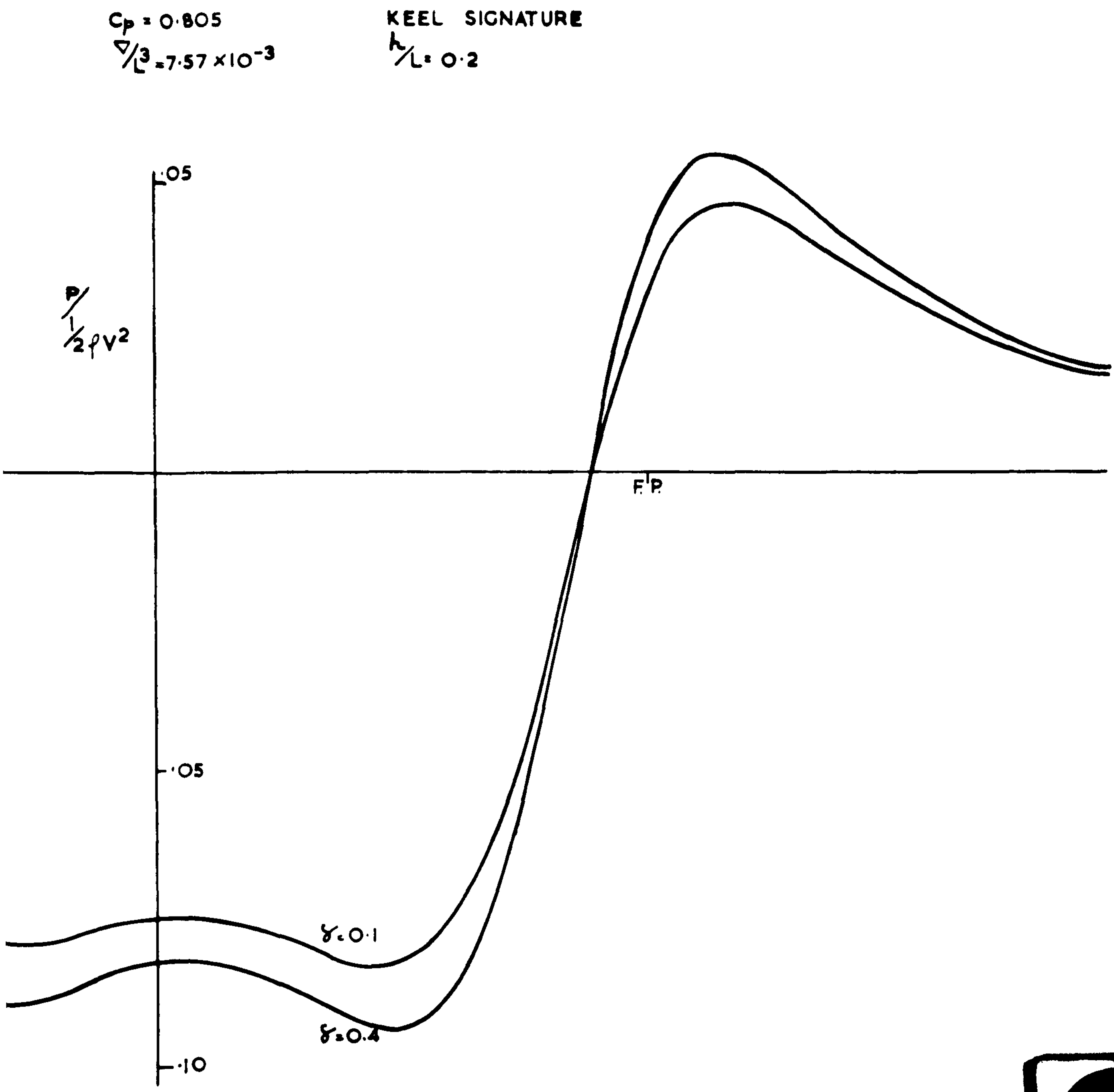

FIG. 10. SERIES 60 KEEL SIGNATURES

SERIES 60 SHIP $C_p = 0 \cdot 805$

$\nabla / L^3 = 7 \cdot 57 \times 1$

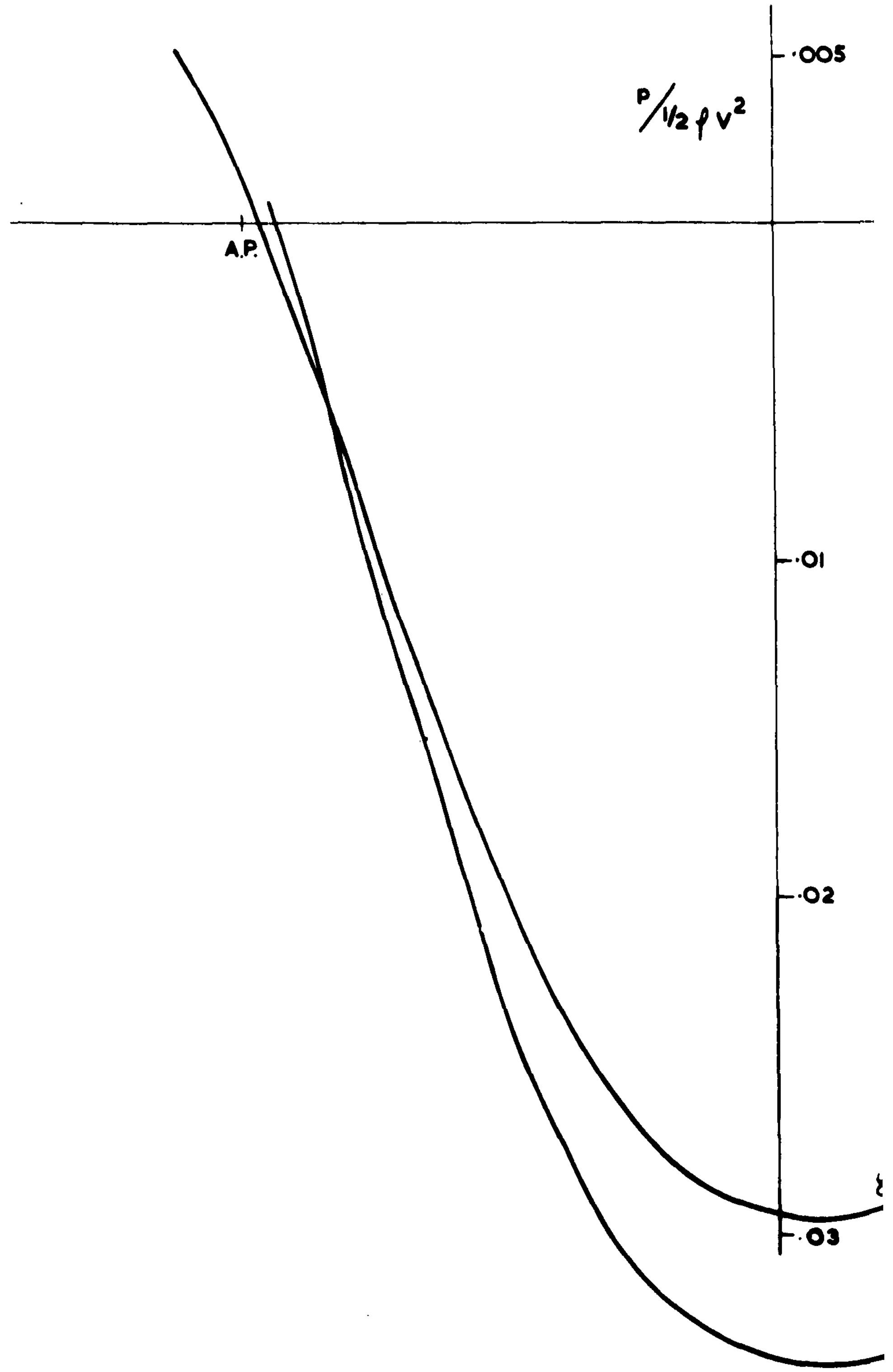

$C_P = 0.805$ KEEL SIGNATURES

$\nabla / L^3 = 7.57 \times 10^{-3}$ $\frac{h}{L} = 0.4$

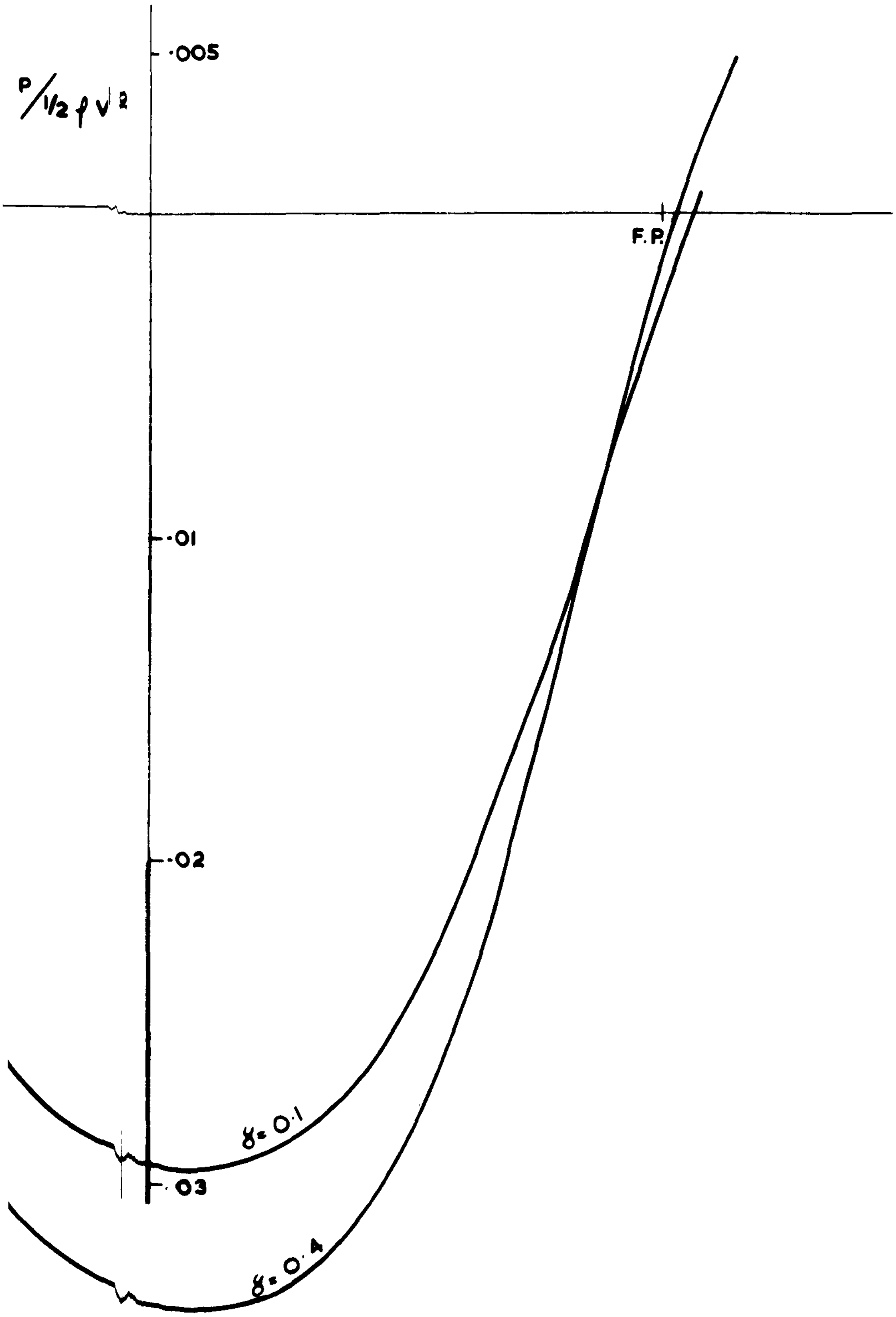

FIG. 11. SERIES 60 KEEL SIGNATURES.

SERIES 60 SHIP $C_p = 0 \cdot 805$ $\nabla / L^3 = 7 \cdot 57 \times 10^{-3}$ KEEL S $\frac{h}{L}$

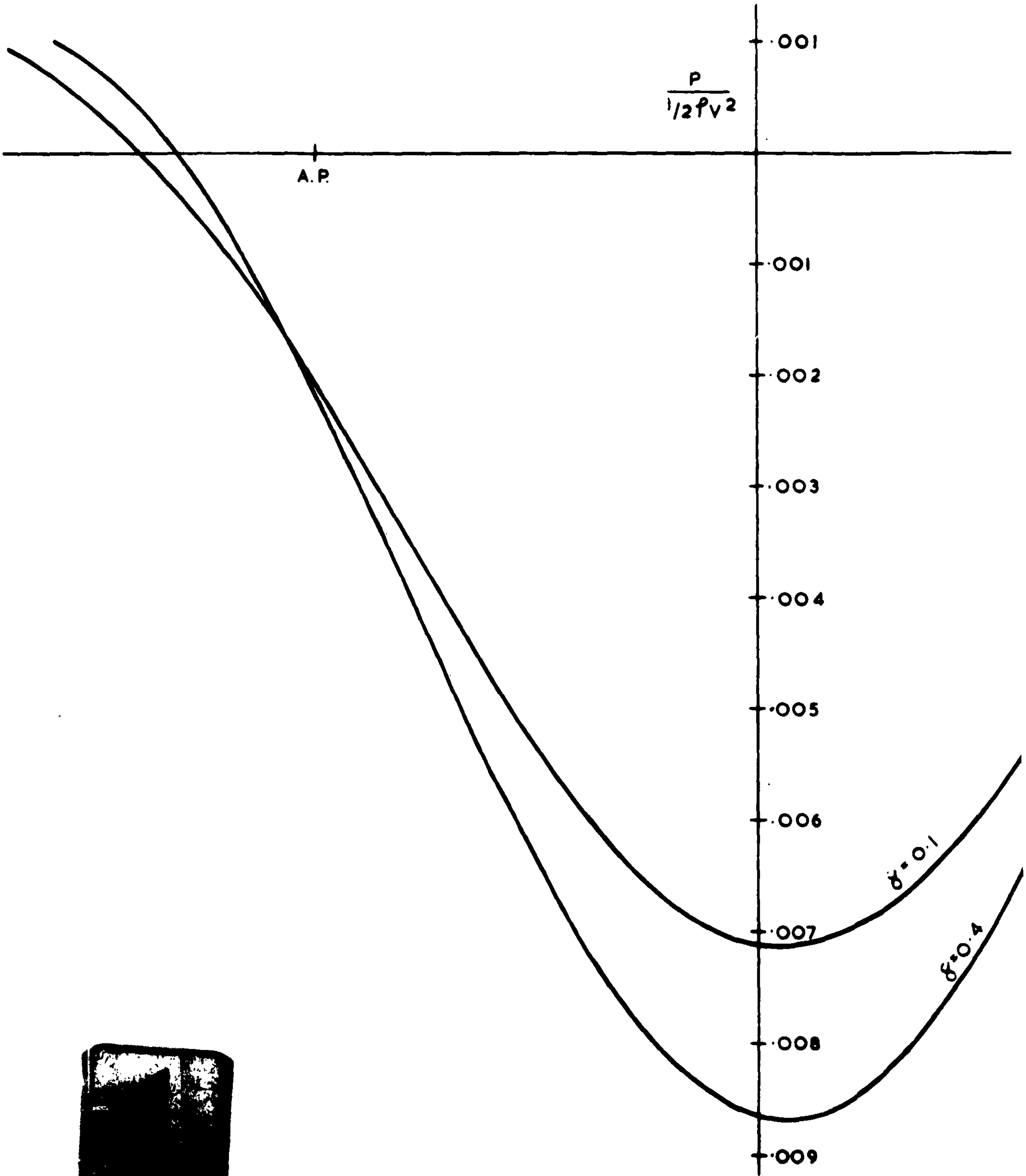

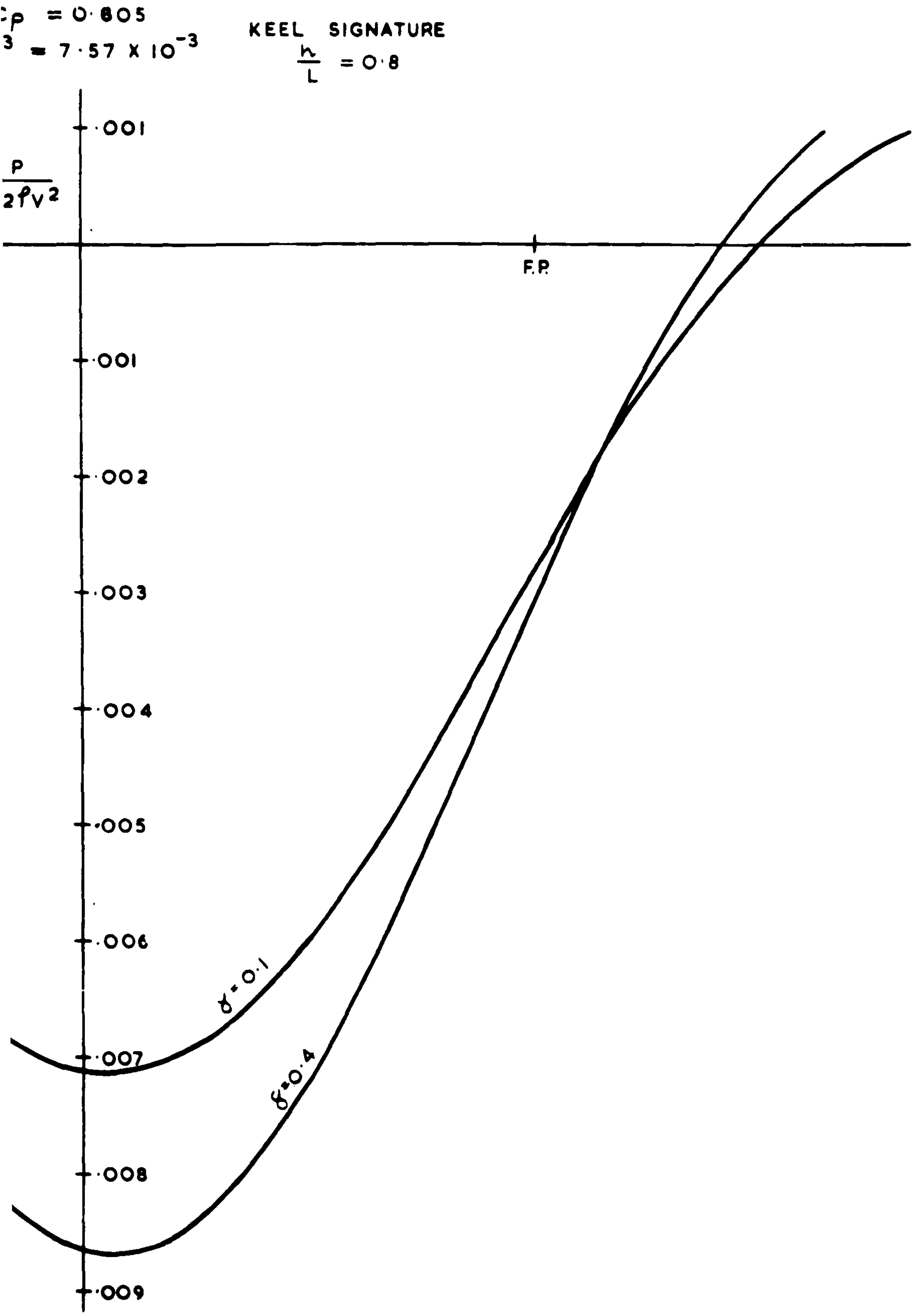

FIG 12. SERIES 60 KEEL SIGNATURES

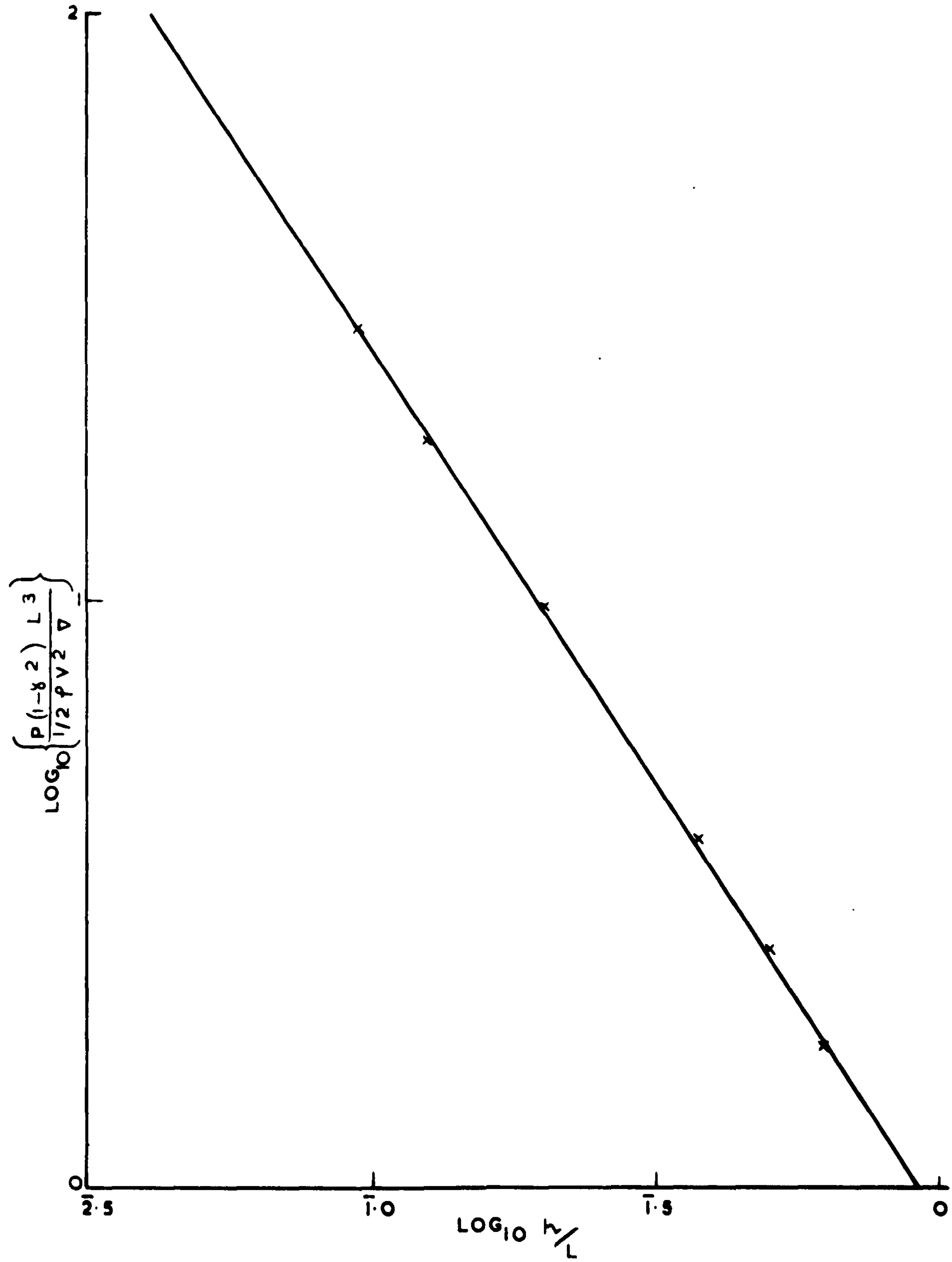

FIG. 13 LOGARITHMIC PLOT
OF A PRESSURE PARAMETER VERSUS RELATIVE DEPTH.
MODEL MERCHANT SHIPS.

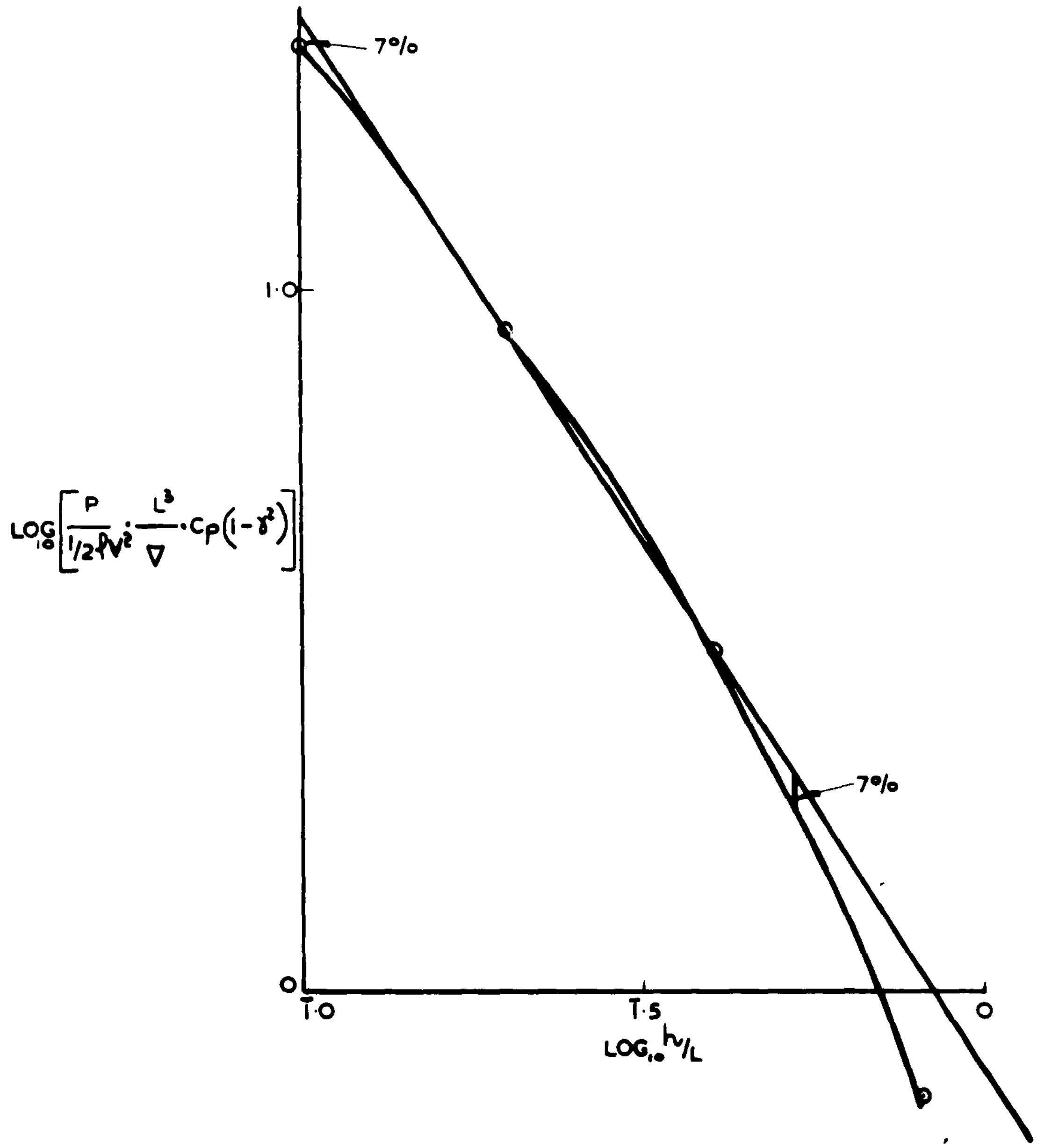

FIG. 14. LOGARITHMIC PLOT OF A PRESSURE PARAMETER VERSUS RELATIVE DEPTH. SERIES 60 SHIPS

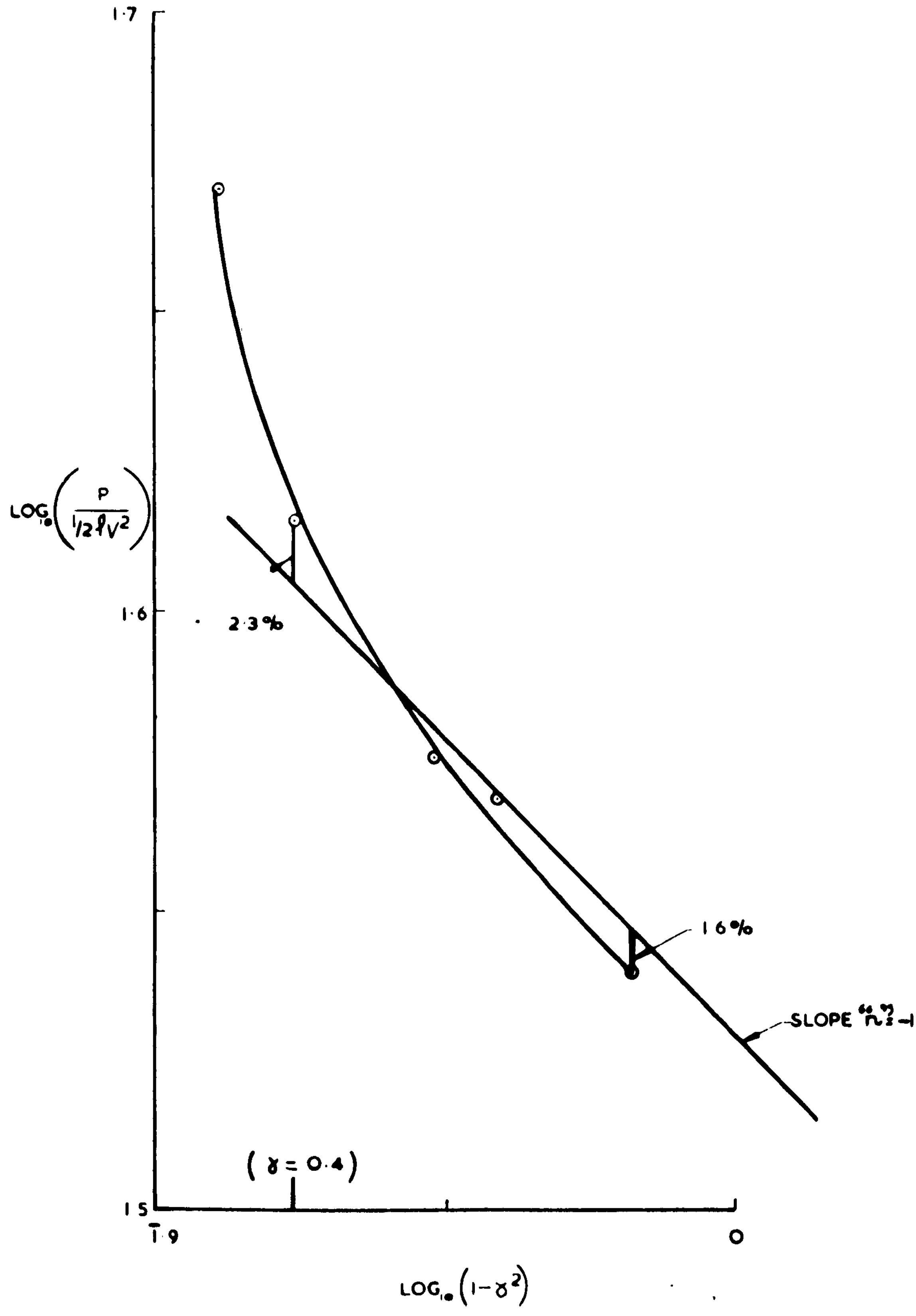

FIG. 15. OBSERVED DEPENDENCE OF P UPON γ FOR A MODEL MERCHANT SHIP

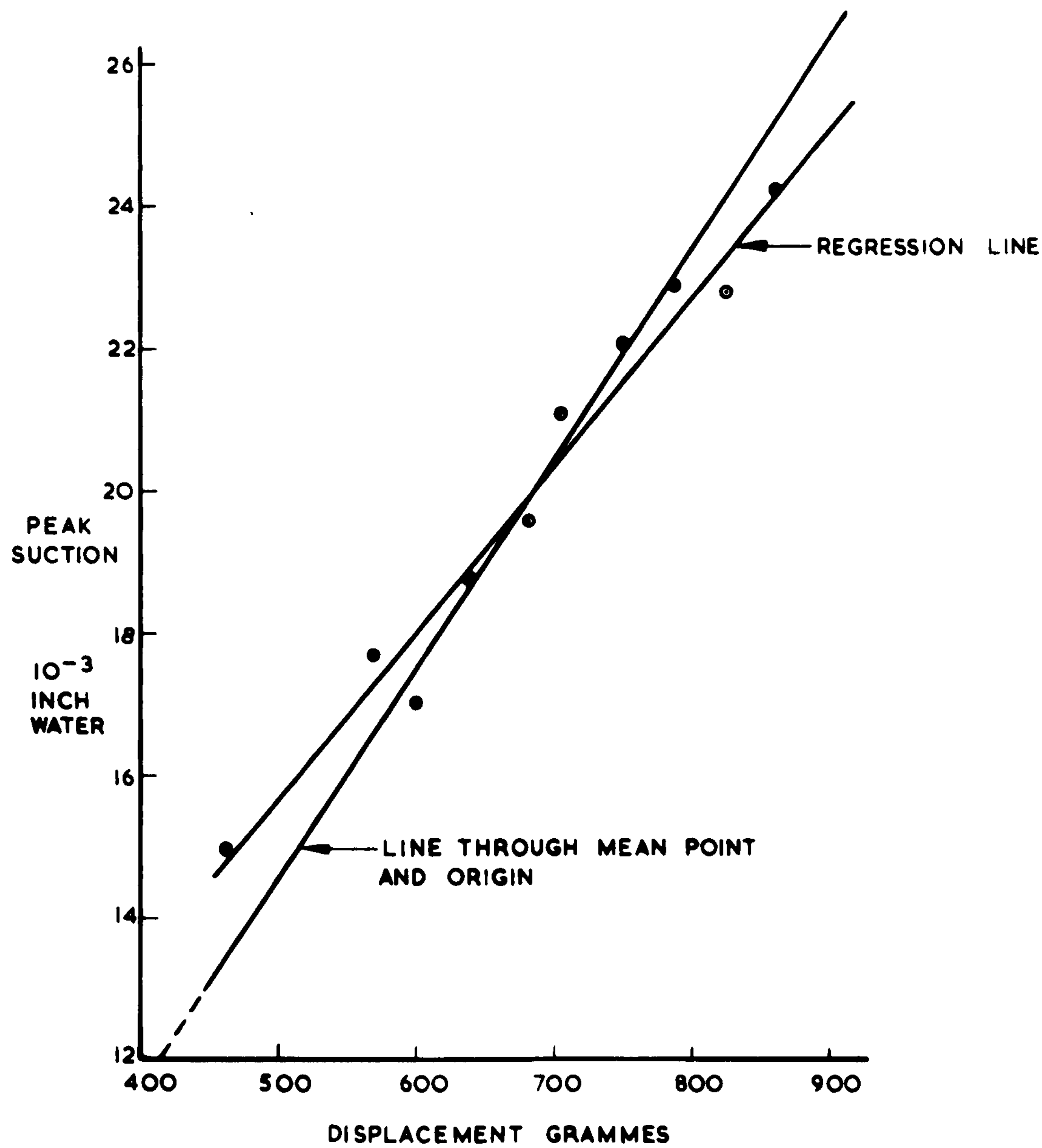

FIG 16. DEPENDENCE OF P ON DISPLACEMENT.

$$\odot \text{-- ORDINATE} = C_P \frac{P(1-\gamma^2)}{\frac{1}{2}\rho V^2} \frac{L^3}{\nabla} \left(\frac{h}{L}\right)^{3/2}$$

$$\times \text{-- ORDINATE} = C_P^2 \frac{P(1-\gamma^2)}{\frac{1}{2}\rho V^2} \frac{L^3}{\nabla} \left(\frac{h}{L}\right)^{3/2}$$

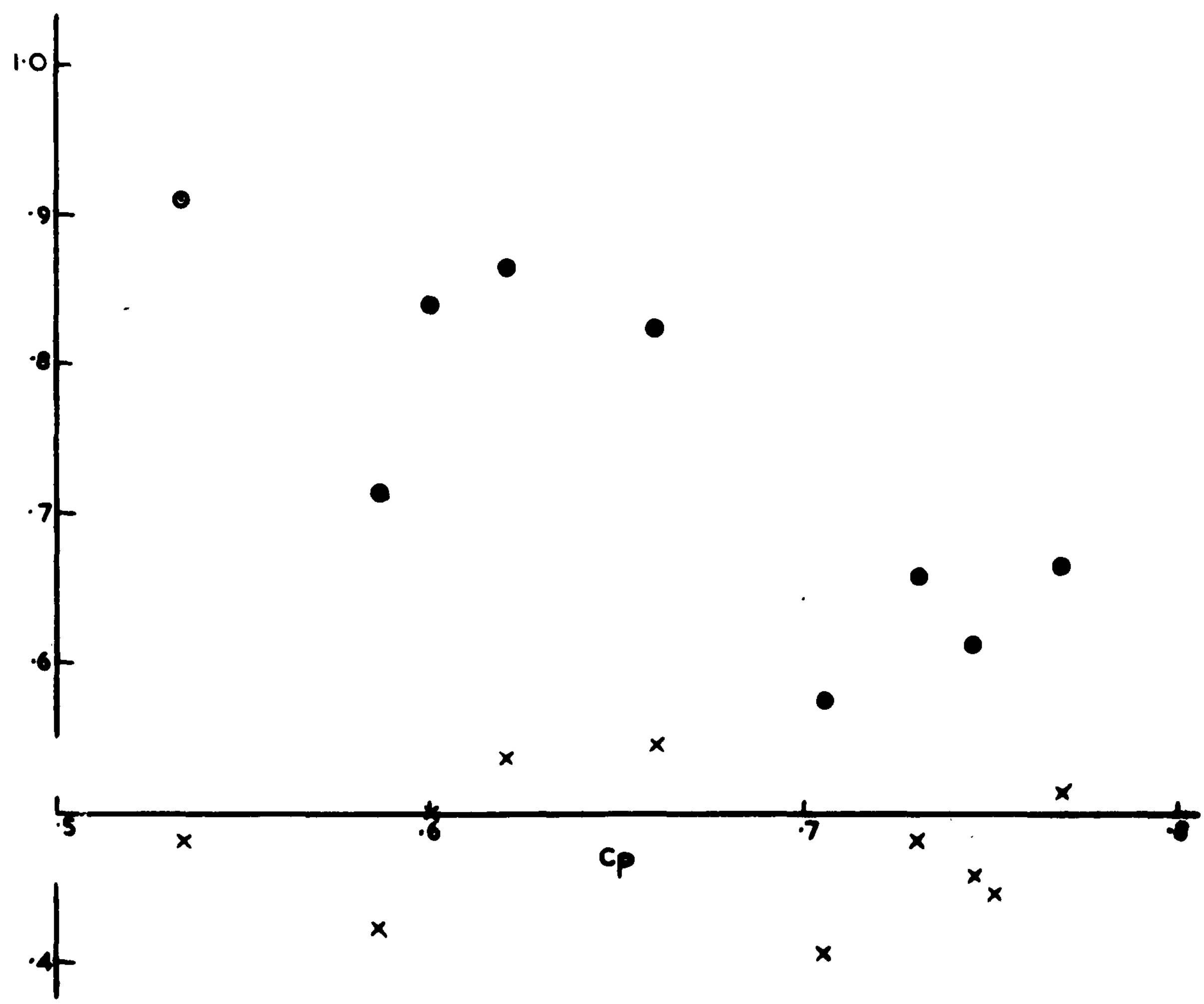

FIG. 17. ILLUSTRATING A MISLEADING APPARENT C_P^2 LAW

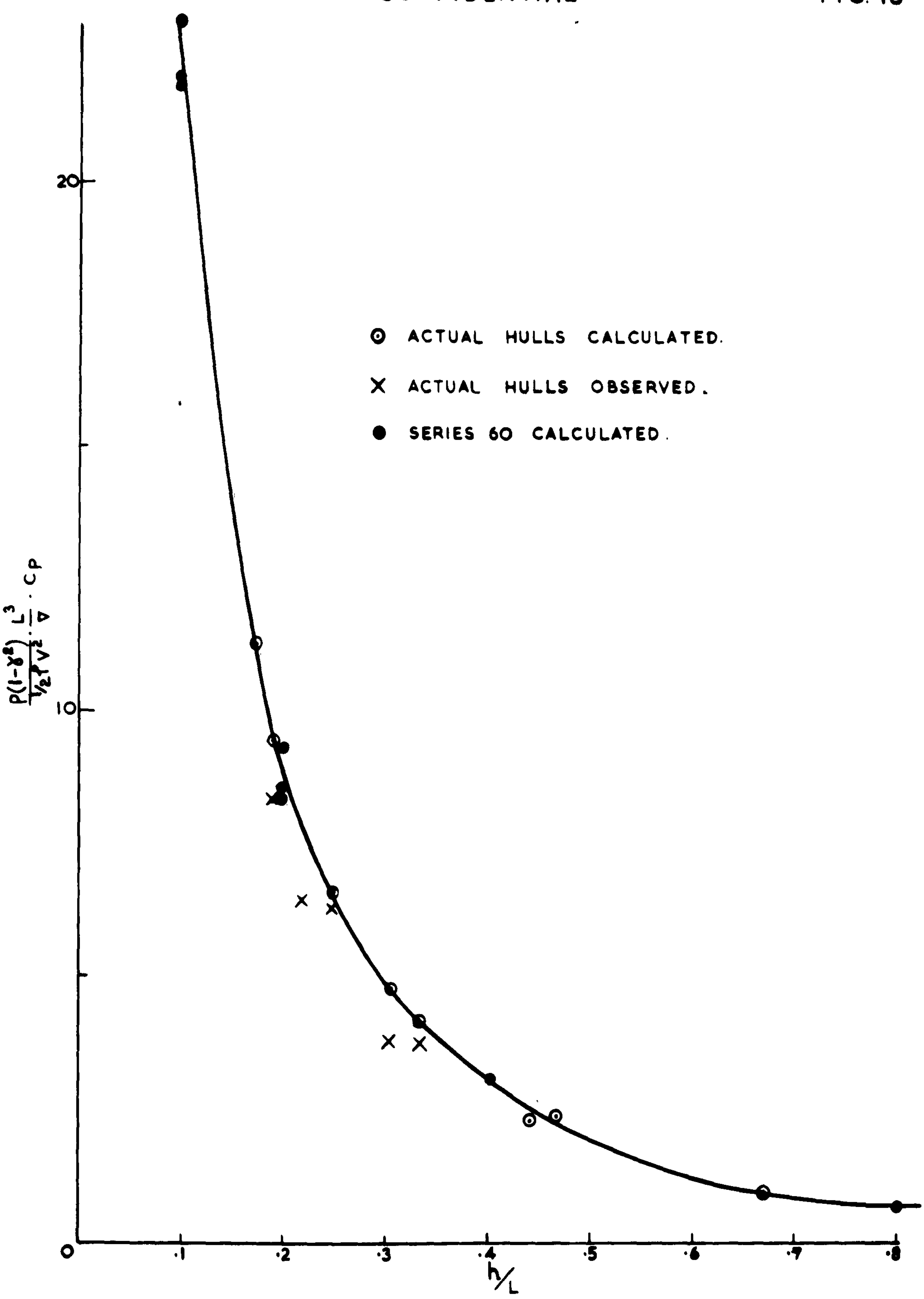

FIG. 18. A PRESSURE NUMERIC VERSUS RELATIVE DEPTH.

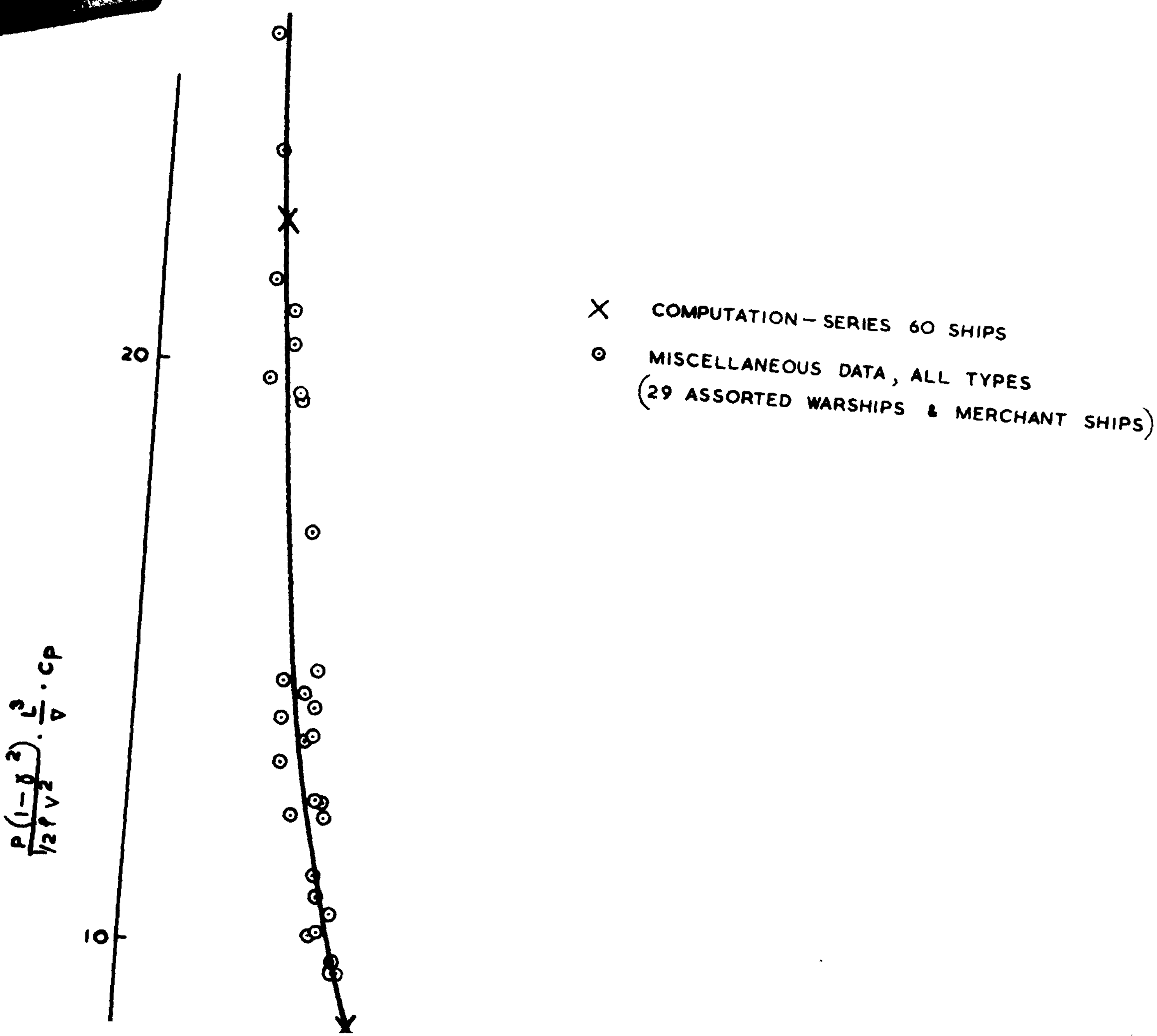

$\frac{P(1-\delta^2)}{1/2 \rho V^2} \cdot \frac{L^3}{\Delta} \cdot C_P$
20
10
× COMPUTATION – SERIES 60 SHIPS
⊙ MISCELLANEOUS DATA, ALL TYPES
(29 ASSORTED WARSHIPS & MERCHANT SHIPS)

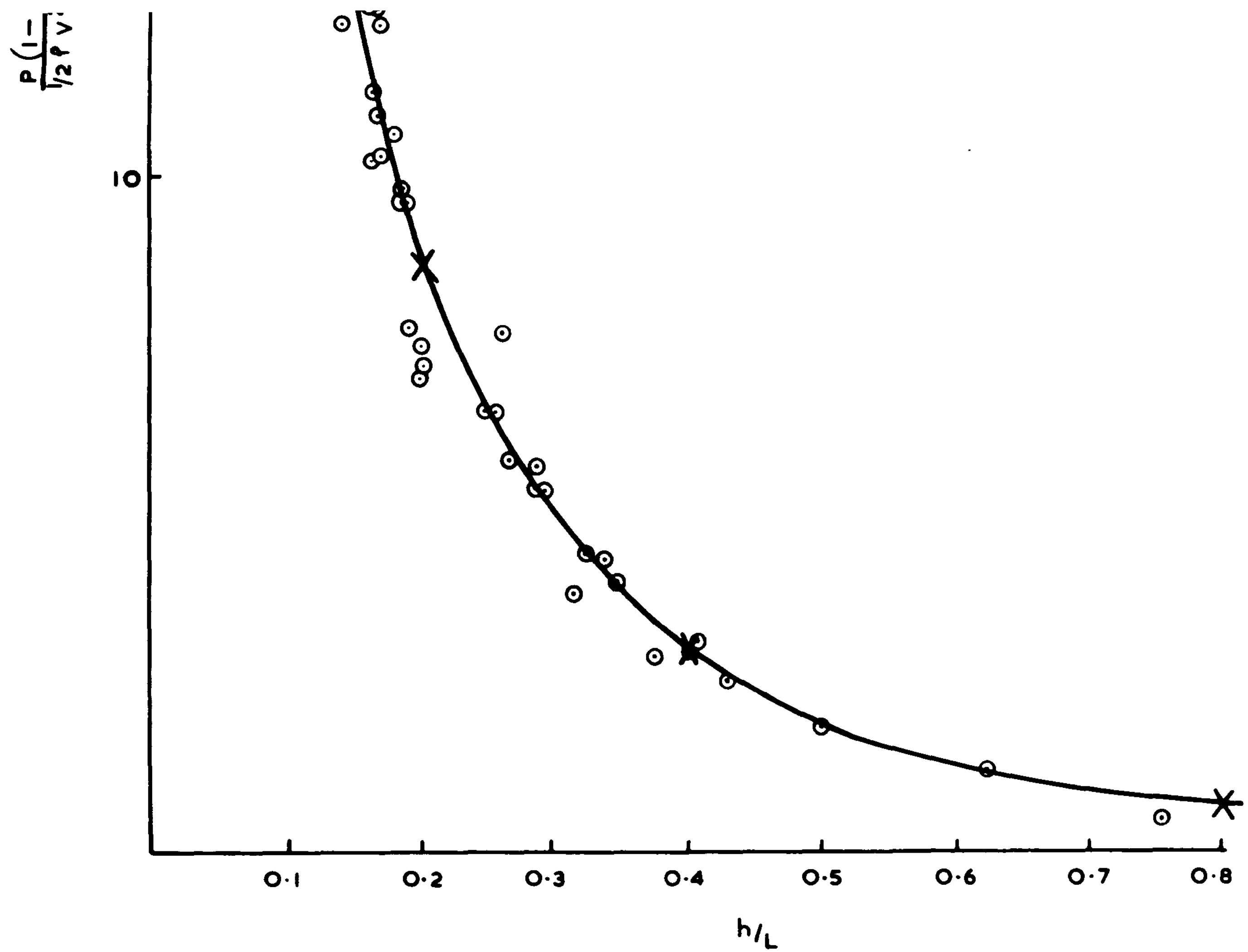

FIG. 19. UNIVERSAL CURVE CONNECTING A PARAMETER BASED ON PEAK SUCTION WITH THE RELATIVE DEPTH.

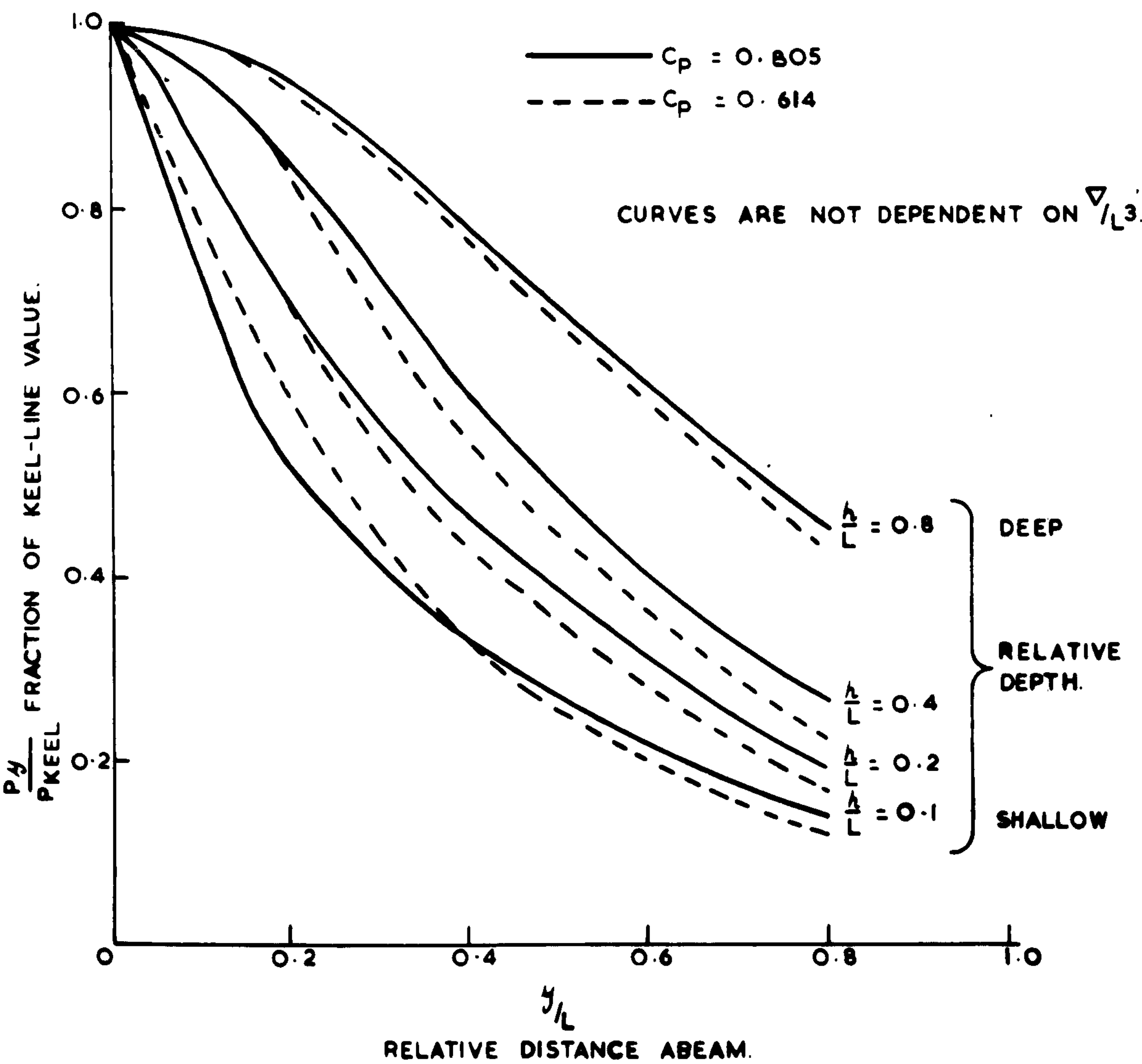

FIG. 20. CURVES SHOWING VARIATION OF PEAK SUCTION WITH DISTANCE ABEAM AT VARIOUS DEPTHS. SERIES 60.

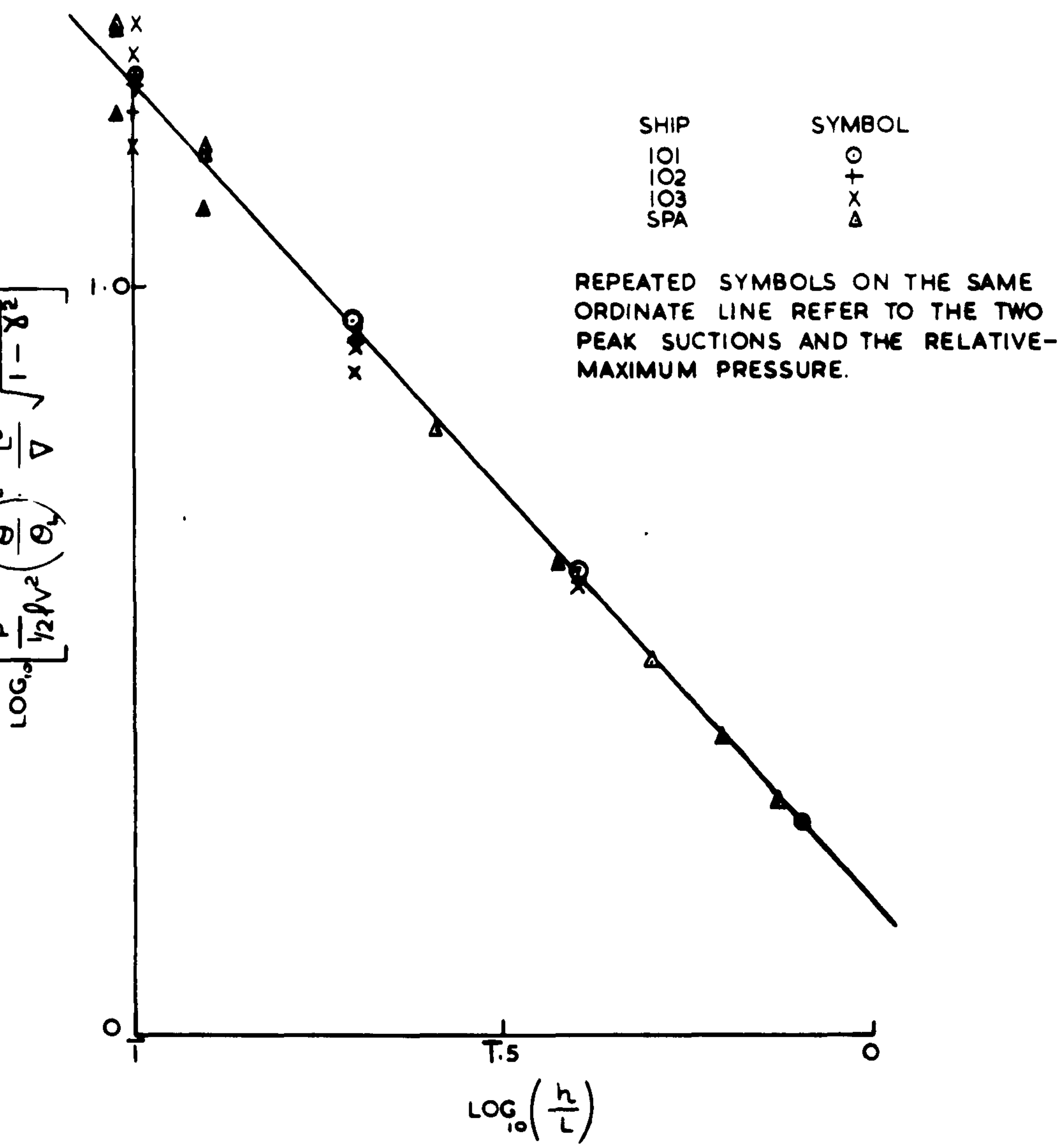

FIG. 21. VARIATION OF DIMENSIONLESS $p\theta^2$ WITH DEPTH RATIO

SERIES 60 $C_p = 0.614$ $\nabla/L^3 = 4.27 \times 10^{-3}$

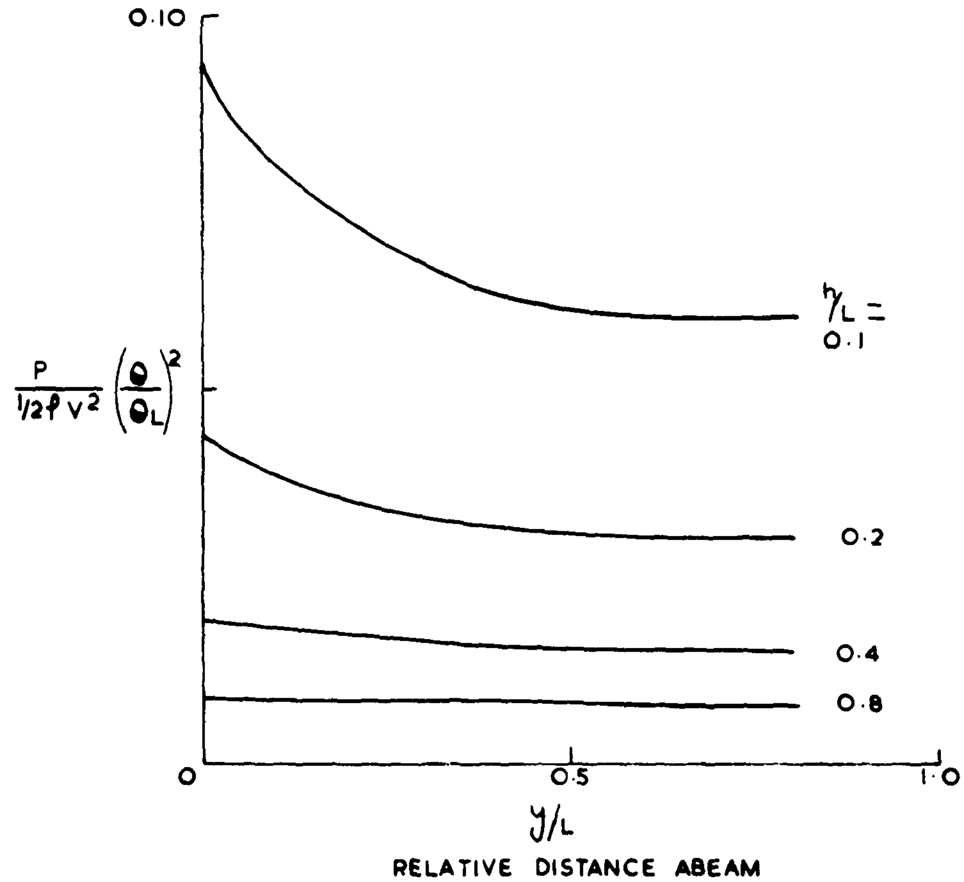

FIG. 22. VARIATION OF DIMENSIONLESS $p\theta^2$ WITH DISTANCE ABEAM

SERIES 60 $C_p = 0.805$ $\nabla/L^3 = 7.57 \times 10^{-3}$
$\gamma = 0.4$

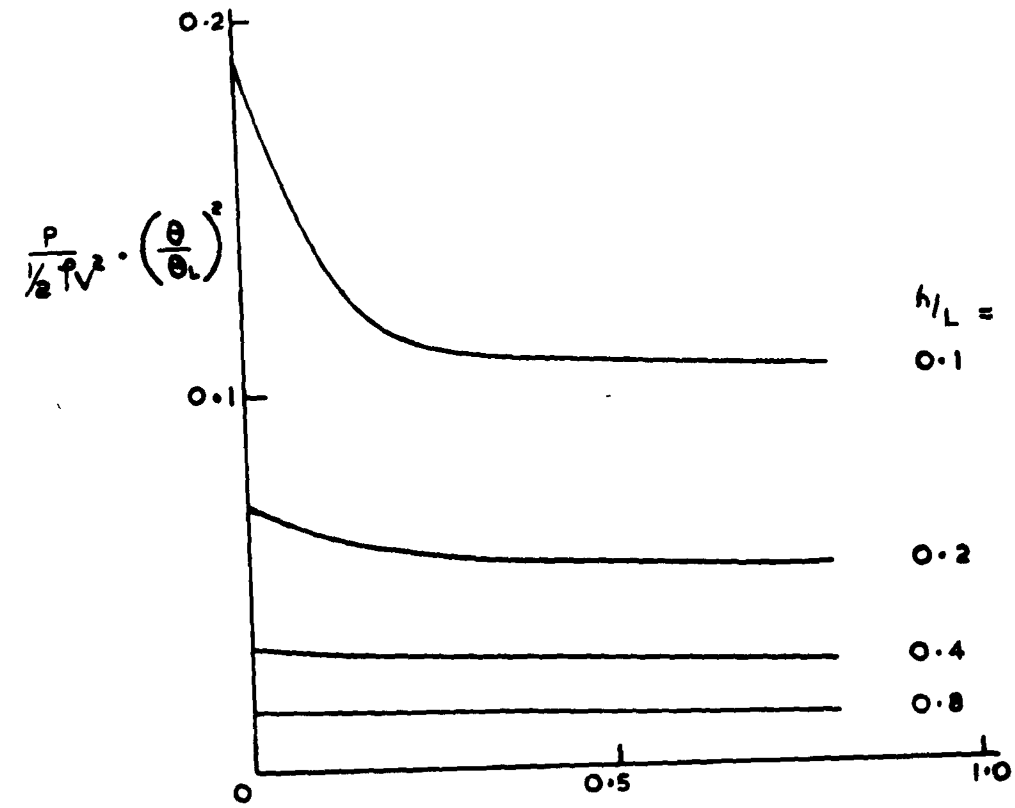

FIG. 23. VARIATION OF DIMENSIONLESS $P\theta^2$ WITH DISTANCE ABEAM

N.A.V. SPA $C_p = 0{\cdot}768$ $\nabla/L^3 = 10{\cdot}22 \times 10^{-3}$

$\gamma = 0{\cdot}4$

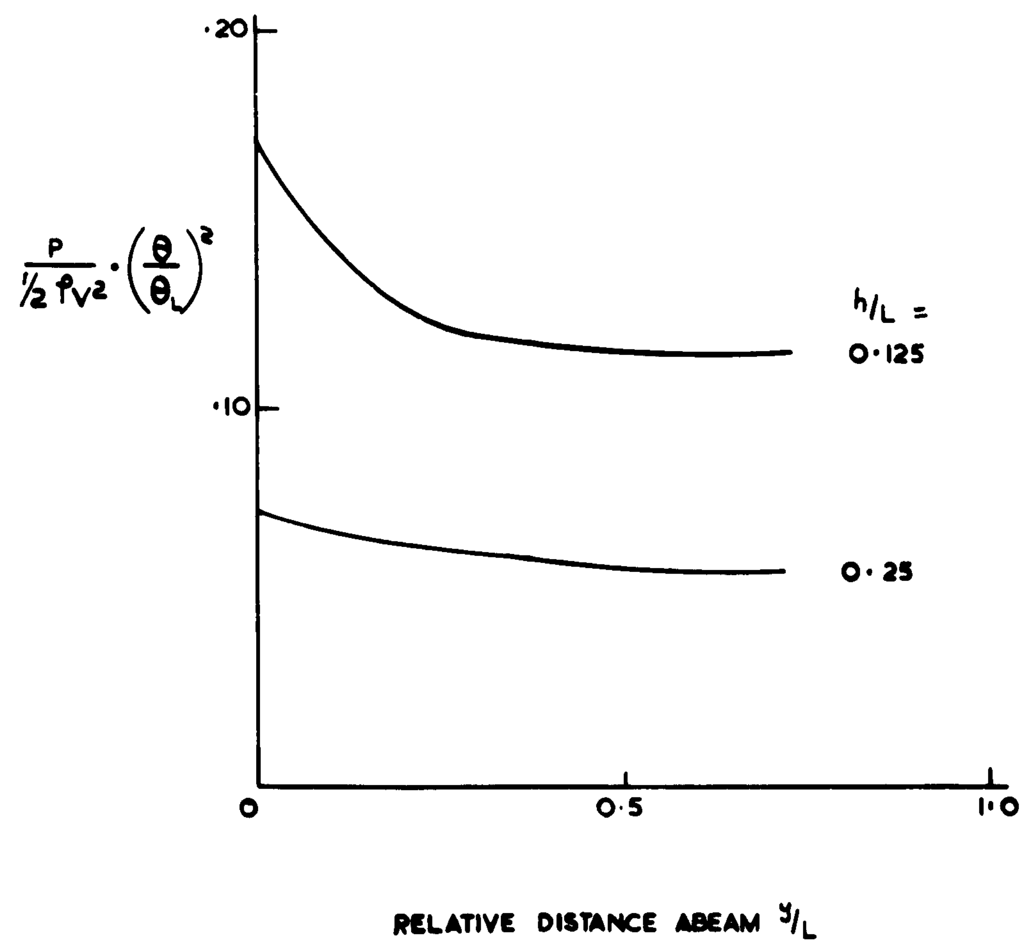

FIG. 24. VARIATION OF DIMENSIONLESS $P\theta^2$ WITH DISTANCE ABEAM

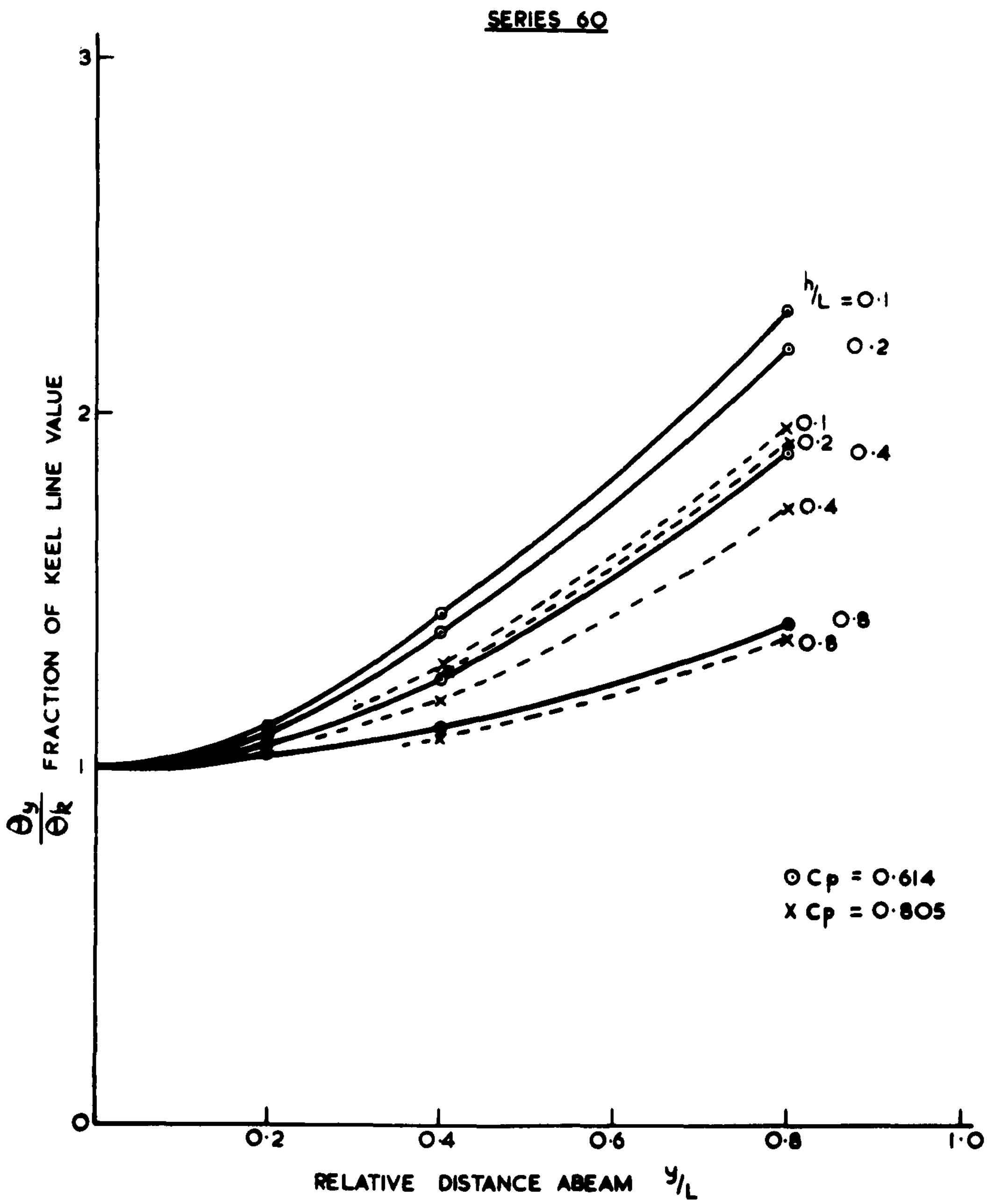

FIG. 25. VARIATION OF TRANSIT TIME WITH DISTANCE ABEAM.

SERIES 60 SHIPS.

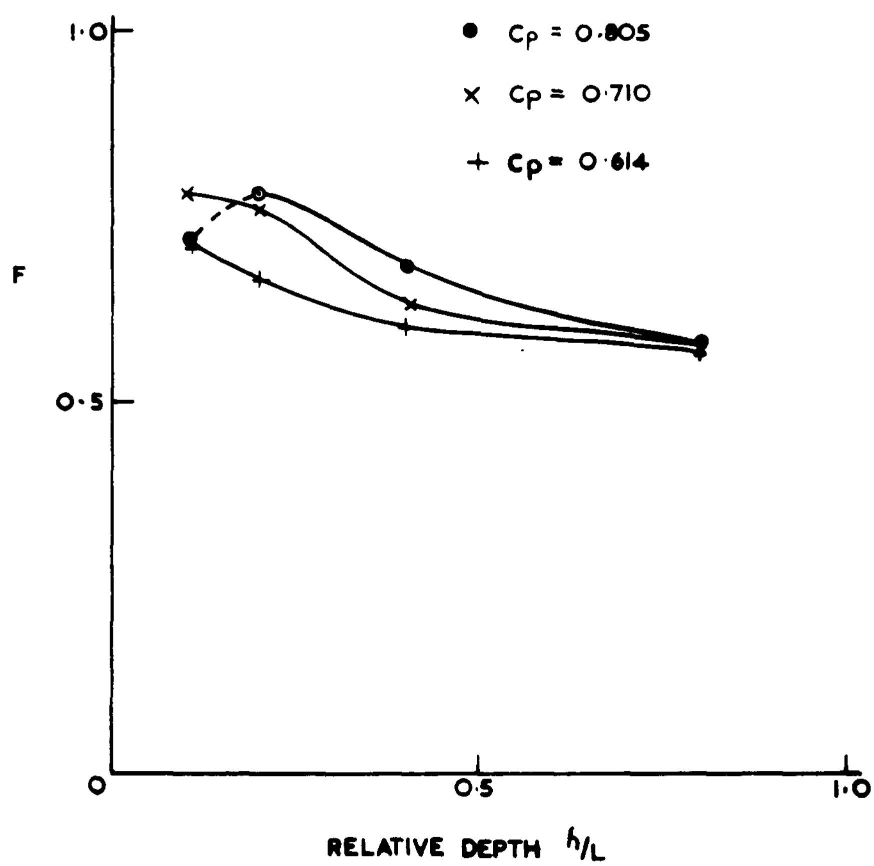

FIG. 26 FULLNESS RATIO VERSUS DEPTH.

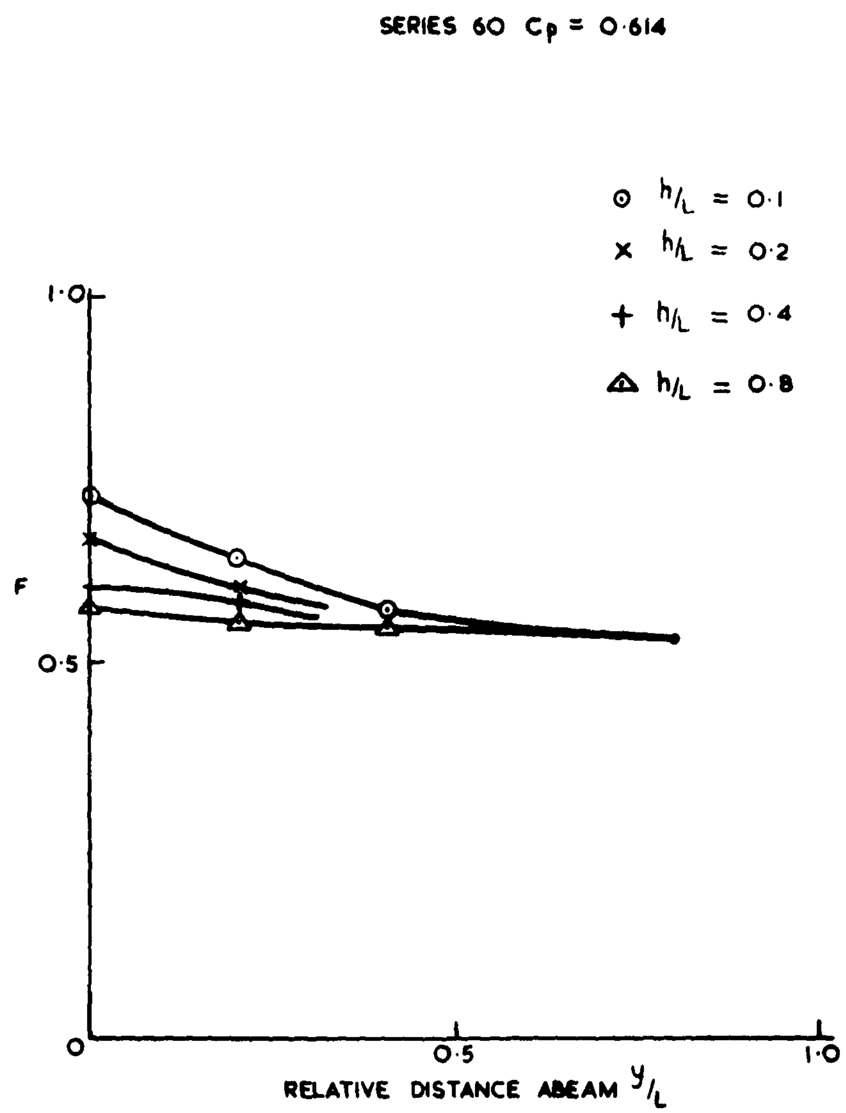

FIG. 27. FULLNESS RATIO VERSUS DISTANCE ABEAM

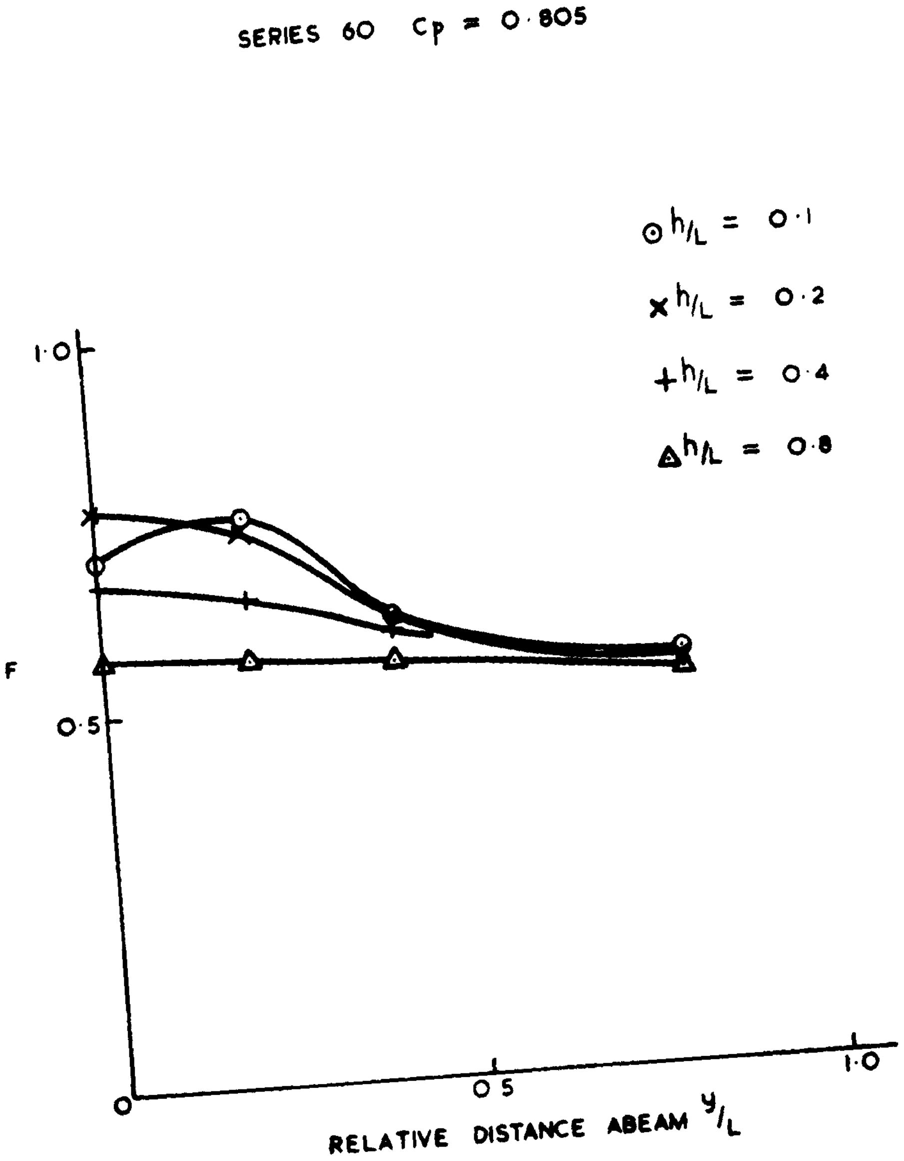

FIG. 28. FULLNESS RATIO VERSUS DISTANCE BEAM

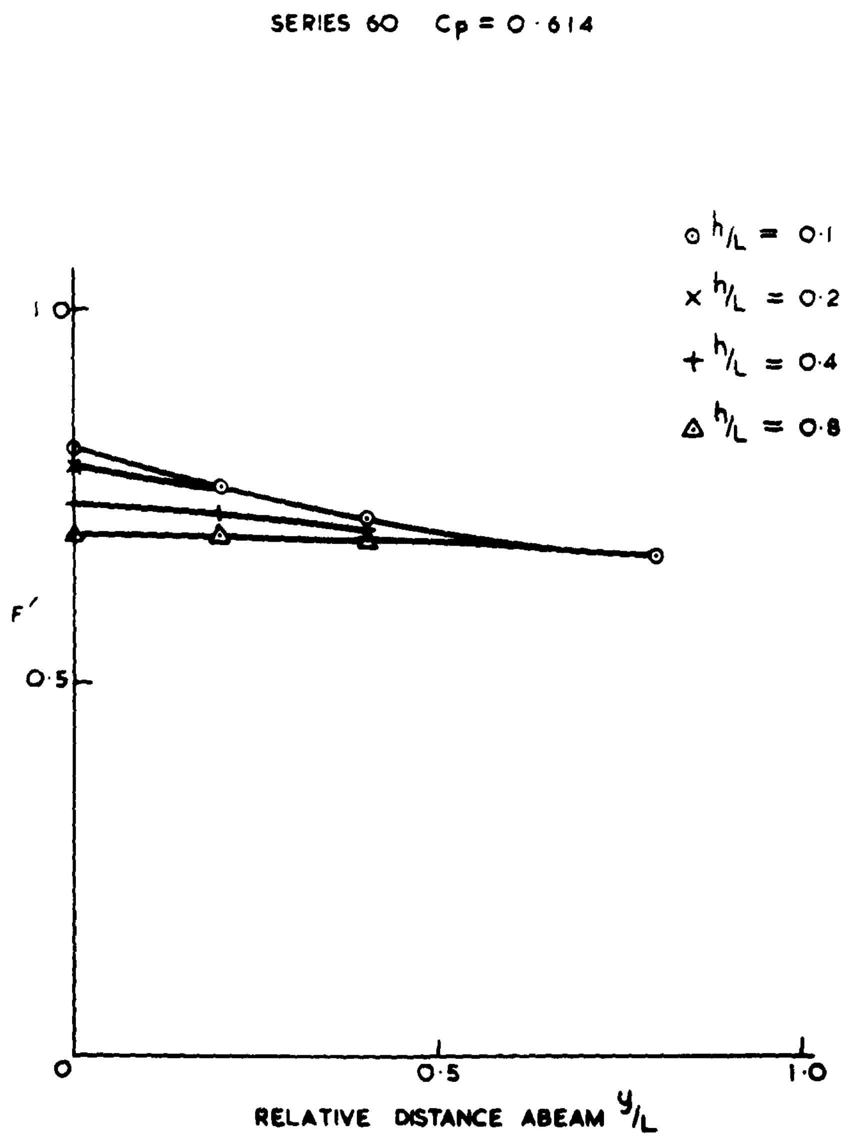

FIG. 29. MODIFIED FULLNESS RATIO VERSUS DISTANCE ABEAM.

CONFIDENTIAL

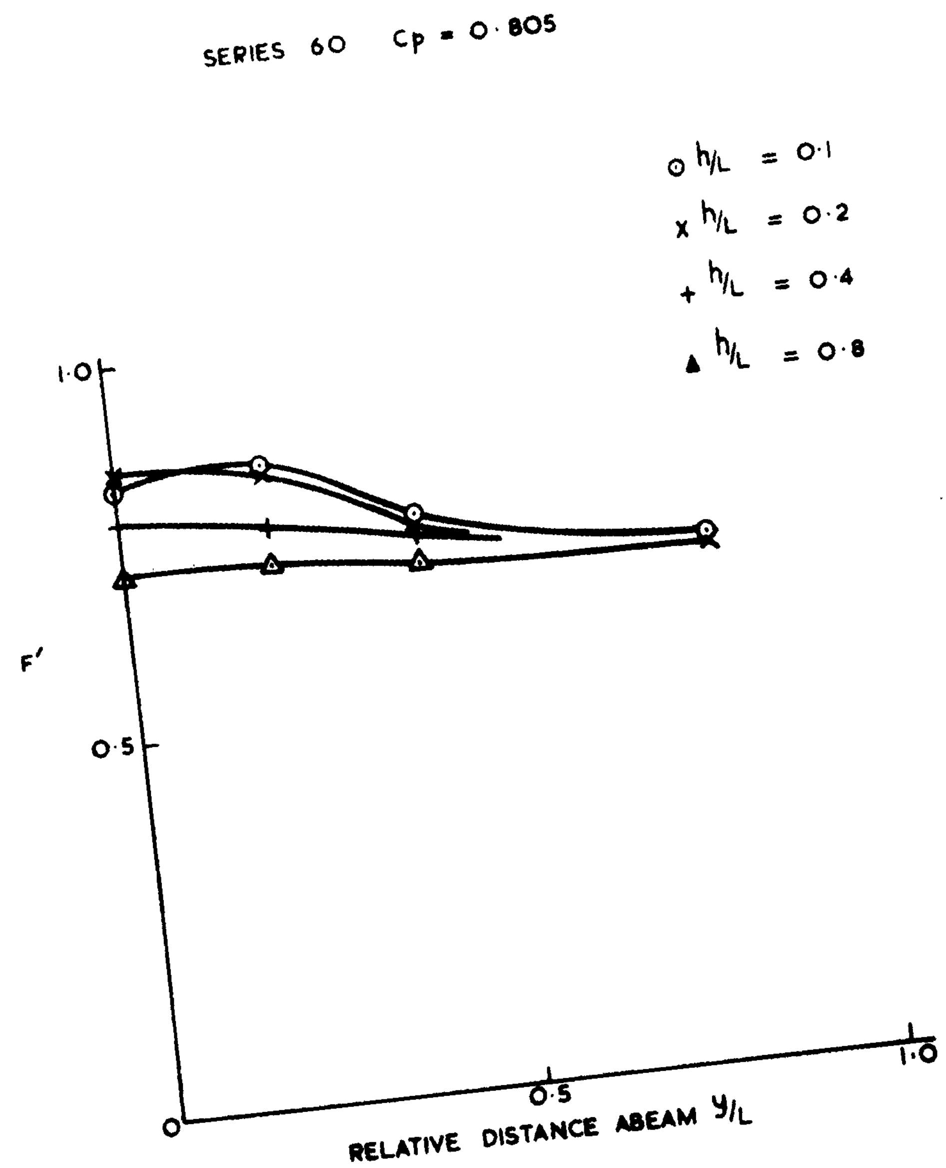

FIG. 30. MODIFIED FULLNESS RATIO VERSUS DISTANCE ABEAM

CONFIDENTIAL

U.K. ABSTRACT
NO.________

(A)	Country of Origin	UNITED KINGDOM
(B)	Establishment of Origin with Short Address	Admiralty Underwater Weapons Establishment, Portland.
(C)	Title of Report	SHIPS' PRESSURE FIELDS
(D)	Author	S. Coad
(E)	Pages and Figures	26 Pages ((i) - (iv) (1 - 22)) 30 Figures
(F)	Date	July 1962
(G)	Originator's Reference	Technical Note No.88/62
(H)	Security Grading	CONFIDENTIAL
(J)	Abstract	Important features of the sea-bed pressure field of a ship are related to two hull-shape parameters, namely the prismatic coefficient and the ratio of displaced volume to length cubed, as well as to speed and depth.

Detachable Abstract Cards

These abstract cards are inserted in A.U.W.E. reports and notes for the convenience of librarians and others who need to maintain an information index

CONFIDENTIAL

A.U.W.E. Technical Note No.88/62 623.863
July 1962
S. Coad

Ships' Pressure Fields

Important features of the sea-bed pressure field of a ship are related to two hull-shape parameters, namely the prismatic coefficient and the ratio of displaced volume to length cubed, as well as to speed and depth.

CONFIDENTIAL

A.U.W.E. Technical Note No.88/62 623.863
July 1962
S. Coad

Ships' Pressure Fields

Important features of the sea-bed pressure field of a ship are related to two hull-shape parameters, namely the prismatic coefficient and the ratio of displaced volume to length cubed, as well as to speed and depth.

CONFIDENTIAL

A.U.W.E. Technical Note No.88/62 623.863
July 1962
S. Coad

Ships' Pressure Fields

Important features of the sea-bed pressure field of a ship are related to two hull-shape parameters, namely the prismatic coefficient and the ratio of displaced volume to length cubed, as well as to speed and depth.

CONFIDENTIAL

A.U.W.E. Technical Note No.88/62 623.863
July 1962
S. Coad

Ships' Pressure Fields

Important features of the sea-bed pressure field of a ship are related to two hull-shape parameters, namely the prismatic coefficient and the ratio of displaced volume to length cubed, as well as to speed and depth.

dstl

Information Centre
Knowledge Services
dstl Porton Down,
Salisbury
Wilts
SP4 0JQ
22060-6218
Tel: 01980-613753
Fax 01980-613970

Defense Technical Information Center (DTIC)
8725 John J. Kingman Road, Suit 0944
Fort Belvoir, VA 22060-6218
U.S.A.

AD#: AD334089

Date of Search: 18 November 2008

Record Summary: ADM 302/88
Title: Ships' pressure fields
Availability Open Document, Open Description, Normal Closure before FOI Act: 30 years
Former reference (Department) AUWE Technical Note 88/62
Held by The National Archives, Kew

This document is now available at the National Archives, Kew, Surrey, United Kingdom.

DTIC has checked the National Archives Catalogue website (http://www.nationalarchives.gov.uk) and found the document is available and releasable to the public.

Access to UK public records is governed by statute, namely the Public Records Act, 1958, and the Public Records Act, 1967.
The document has been released under the 30 year rule.
(The vast majority of records selected for permanent preservation are made available to the public when they are 30 years old. This is commonly referred to as the 30 year rule and was established by the Public Records Act of 1967).

This document may be treated as <u>UNLIMITED</u>.